ICMAB

INSTITUT DE CIÈNCIA DE
MATERIALS DE BARCELONA

Xavier Obradors
Director ICMAB – CSIC

CONSEJO SUPERIOR DE INVESTIGACIONES CIENTÍFICAS

Where are we?

Bellaterra campus (Univ. Aut. Barcelona, 20 km)

ICMAB RESEARCH ACTIVITIES

CSIC

ICMAB

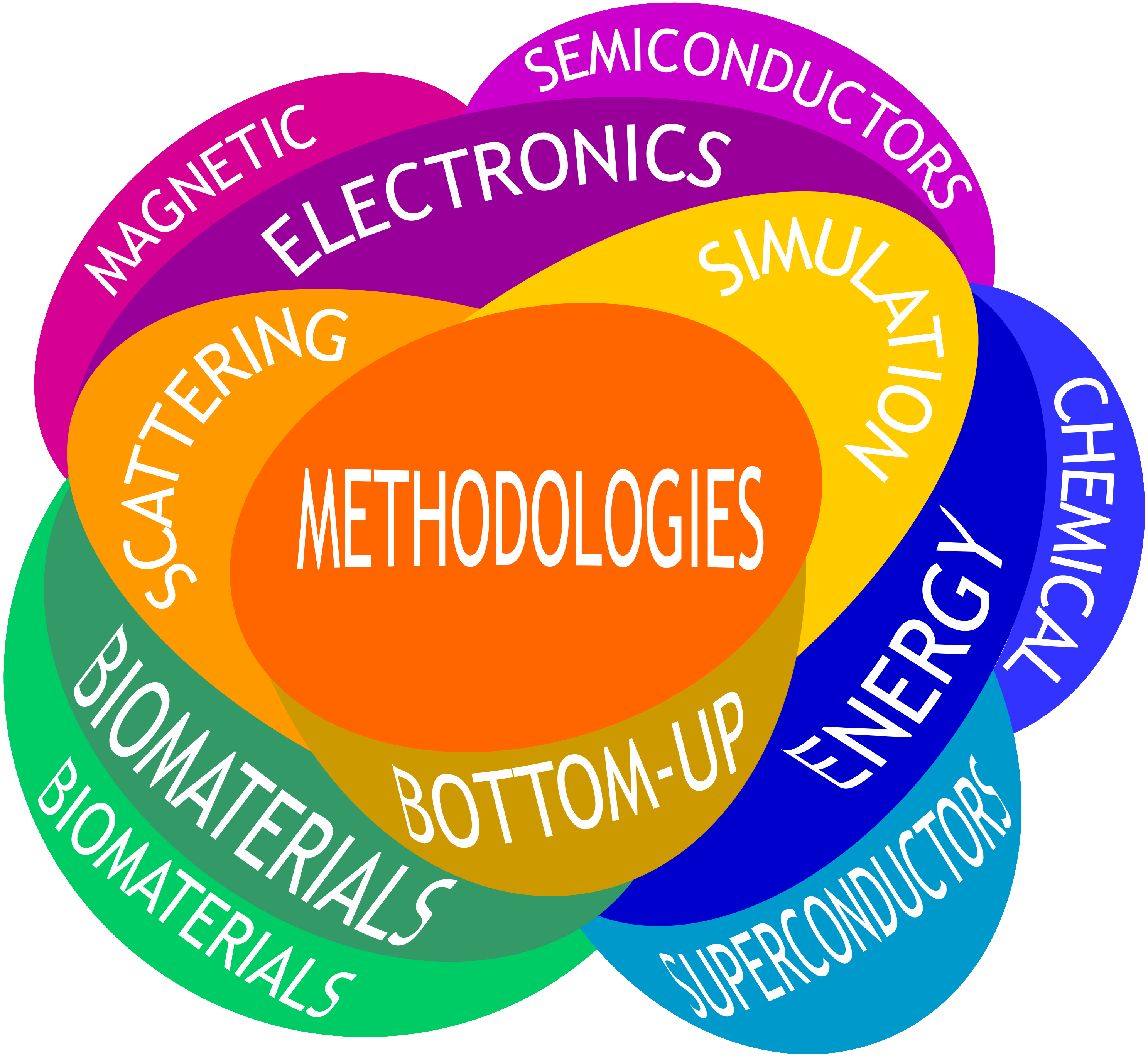
SEMICONDUCTORS
MAGNETIC
ELECTRONICS
SIMULATION
SCATTERING
METHODOLOGIES
CHEMICAL
ENERGY
BOTTOM-UP
BIOMATERIALS
BIOMATERIALS
SUPERCONDUCTORS

CSIC

ICMAB

Battery materials

Energy Research

New materials, alternative mechanisms

PCT application ES03/00249
J. Electrochem. Soc. 152(11), (2005)
Inorg. Chem. (submitted)

$M_xO_y + 2y\,Li^+ \rightarrow y\,Li_2O + x\,M + 2y\,e^-$

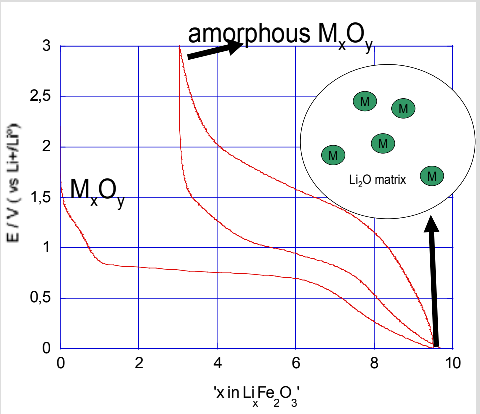

High T batteries

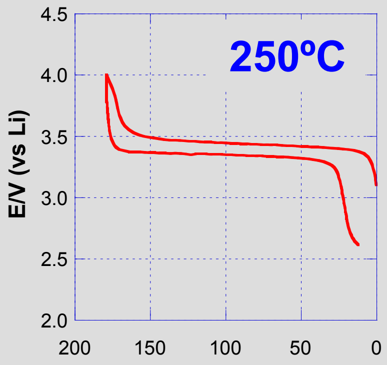

Electrochem. Comm. 9, 708 (2007))

Correlation microstructure-electrochemical yield

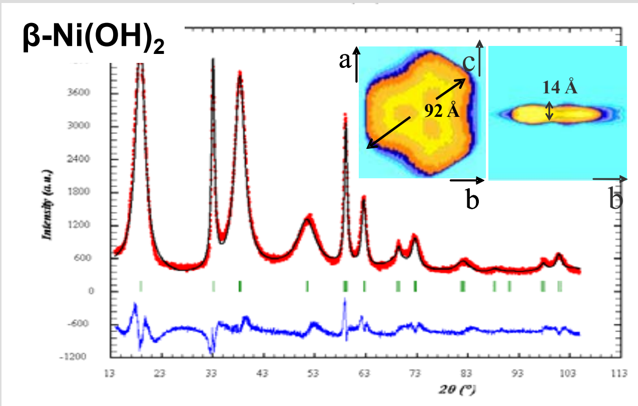

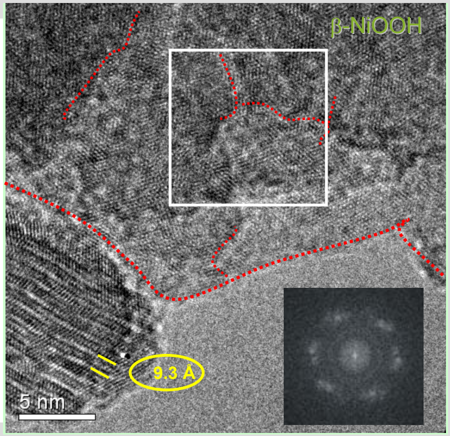

Journal of the American Chemical Society, 129, 5840 (2007)
Journal of Materials Chemistry 16, 2925 (2006)

ALISTORE ERI

Xarxa de Referència en Materials Avançats per a l'Energia
Generalitat de Catalunya

CSIC

ICMAB

Nitride materials with photocatalytical activity in the visible range

Energy Research

Nitrogen doping of oxides decreases the band gap because of the lower electronegativity of N vs O, shifting the photocatalytical activity from the UV to the visible range

Mesoporous nanostructured thin films of $TiO_{2-x-y}N_x$ (anatase)

N1s XPS as a function of the nitriding temperature in NH_3

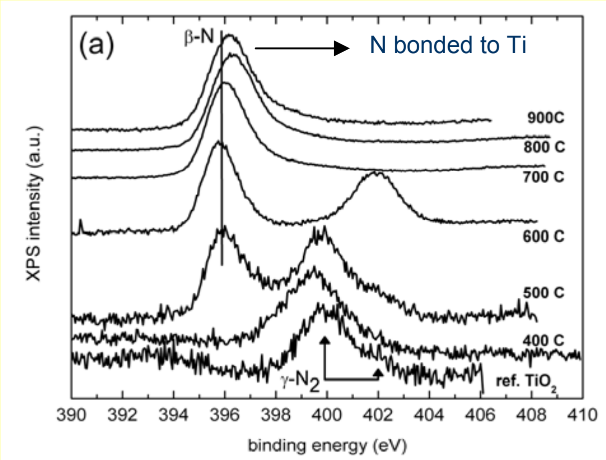

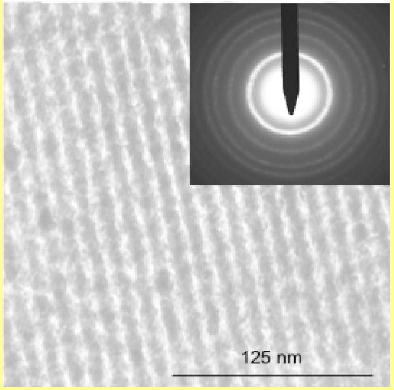

The mesostructure is kept until T=700 °C

Advanced Functional Materials, 17, 3348 (2007)

New nitrogen doped ceria (CeO_2) with photocatalytical activity in the visible range

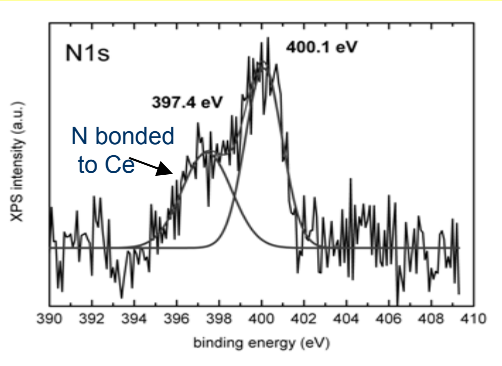

Solid solution $CeO_{2-x-y}N_x$ up to 4.5 mol % N

Rate of CO_2 evolution for decomposition of acetaldehyde as a function of irradiation λ over N-doped CeO_2 films

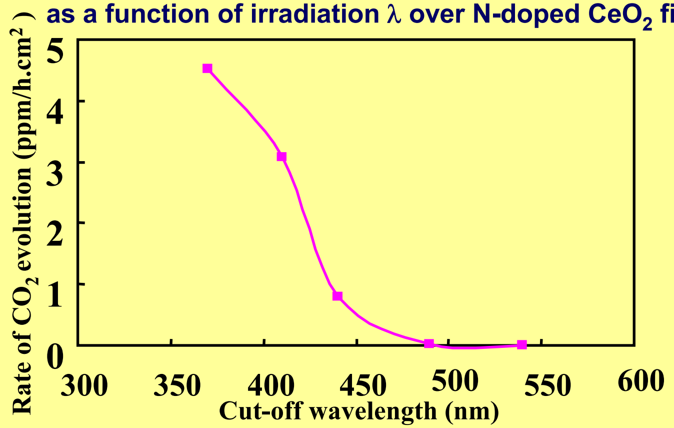

Chemistry of Materials, 2, 1682 (2008)
A.Fuertes, A.B.Jorge. Pat. Esp. 200700482. 23-02-2007.

Hydrogen by Ethanol Reforming

Energy Research

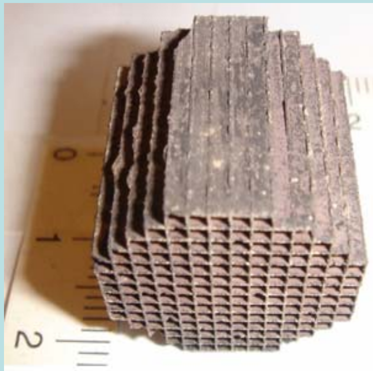

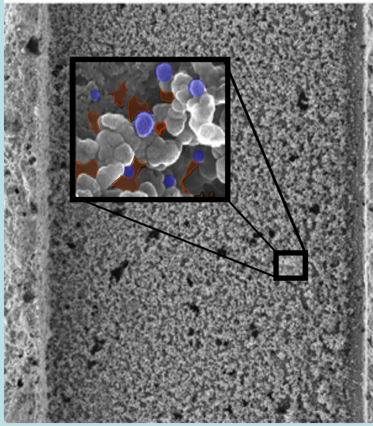

Catalyst grown on cordierite substrate: Nanocomposited silica aerogel with cobalt nanoparticles (blue in the idealized inset).

The catalytic device can be simply heated up to the reaction temperature (320-340ºC) under air, and then the ethanol is introduced for the generation of hydrogen.

$$C_2H_5OH + 3H_2O \rightarrow 6H_2 + 2CO_2$$

This has a strong potential for fuel cell technology as well as for on-board generation of hydrogen for mobile applications.

The catalytic device can be easily operated and doesn't require special care for shut down cycles, thus allowing interrupted and/or oscillating operation for real practical application. No activation and/or conditioning are required for operation.

Co-SiO_2 aerogel-coated catalytic walls for the generation of hydrogen, M.Domínguez, E.Taboada, E.Molins, J.Llorca, Catalysis Today (2008) and CSIC-UPC patent (2007)

Chemical solution approaches to self-assembled and nanocomposite superconducting films

Xavier Obradors

T.Puig, A. Pomar, A. Palau, F. Sandiumenge, S. Ricart, N. Mestres, J. Gutiérrez, M. Gibert, A. Llordés, A. Carretero, C. Moreno, R.F. Luccas, J. Zabaleta, F. Martínez, P. Abellán, N. Romà, A. Benedetti, J. Gázquez, M. Coll, R. Vlad, X.Granados

Institut de Ciència de Materials de Barcelona, CSIC, 08193 Bellaterra, Spain

HIPERCHEM

ESAS
The European Society for Applied Superconductivity

POWER APPLICATIONS SUPERCONDUCTORS

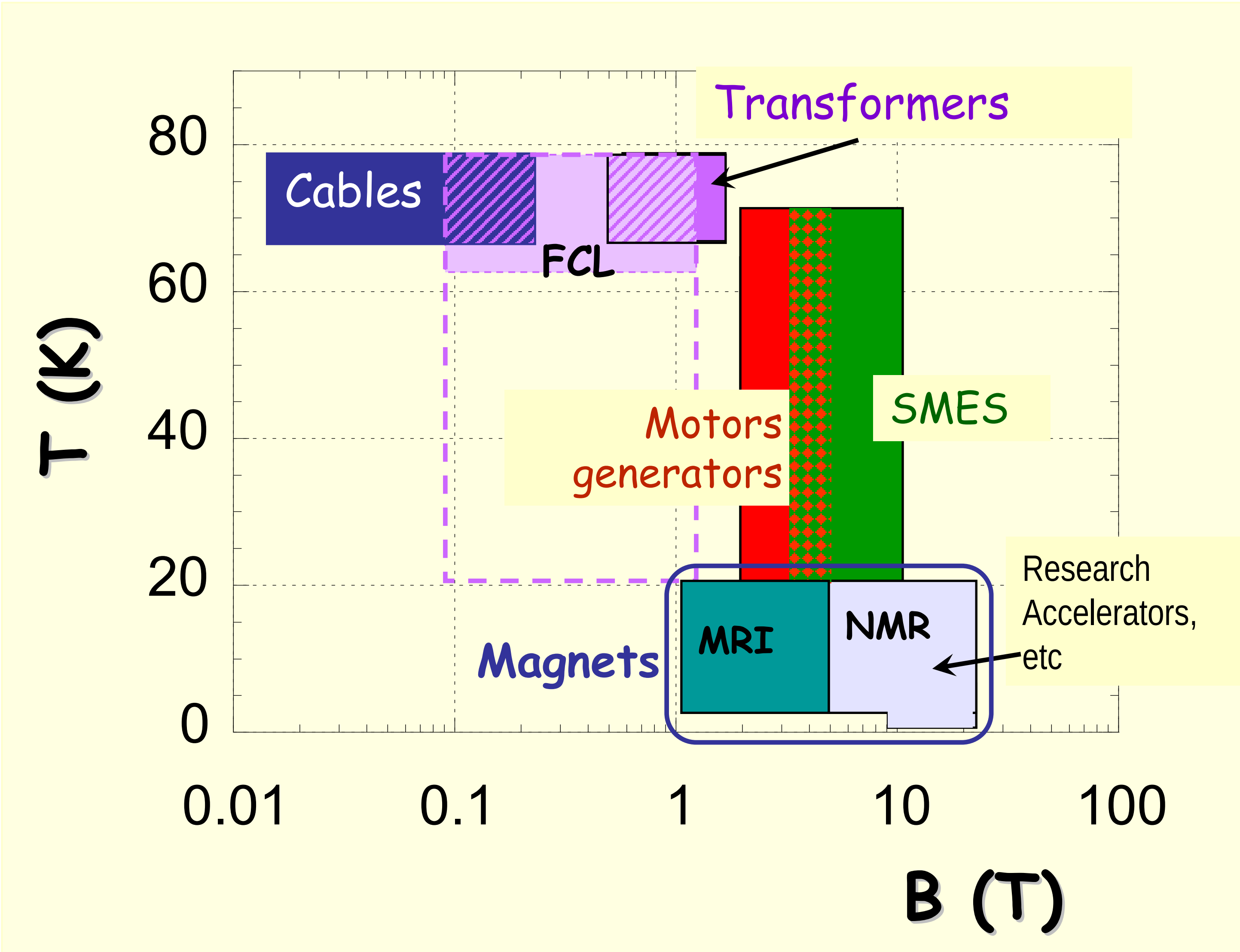

COATED CONDUCTORS ARCHITECTURE

CSIC

ICMAB

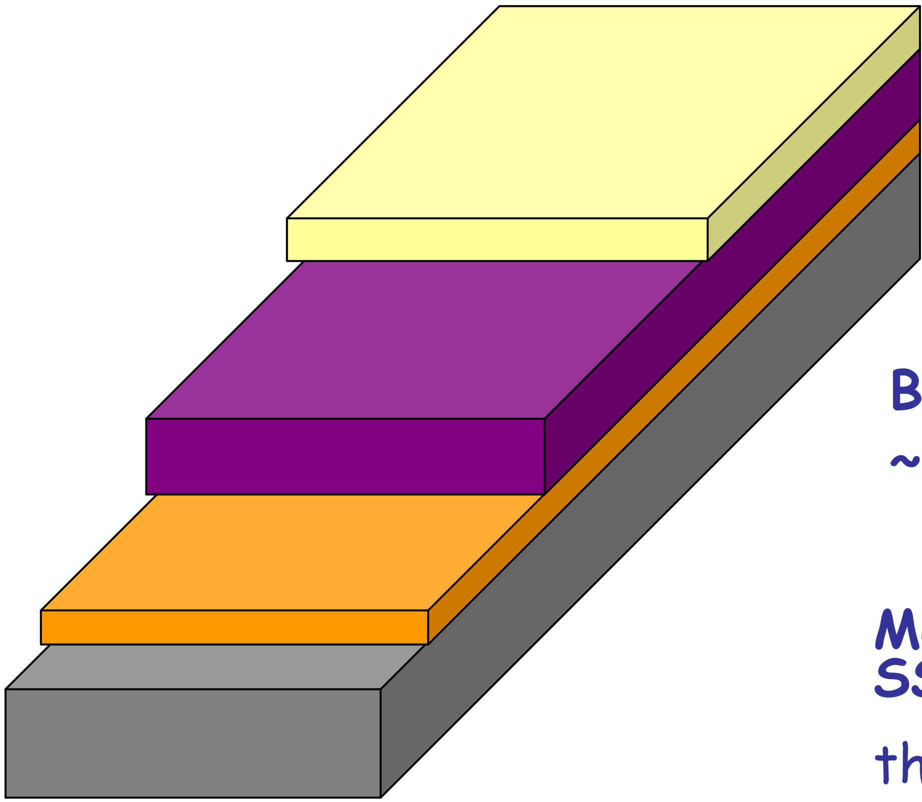

Cap layer : Ag

thickness ≈ 0.2 - 0.5 μm

SC layer : YBCO

~ 1.0 μm

Buffer layers : CeO_2 , YSZ, STO,…

~ 0.1 μm

Metallic substrate: RABiTS Ni, SS-IBAD

thickness ~ 80 μm

Nanostructure control on km length materials

GOALS

- The potentiality and richness of chemical solution methods for growth of nanostructured films and coated conductors:
  - A flexible, scalable and controllable bottom-up approach
- Nanostructured YBCO films by chemical routes
  - Interfacial nanostructured films
  - Nanocomposites
  - Ferromagnetic-superconductor nanostructured YBCO films
- Methodology to analyze vortex pinning based on angular dependent transport J_c measurements

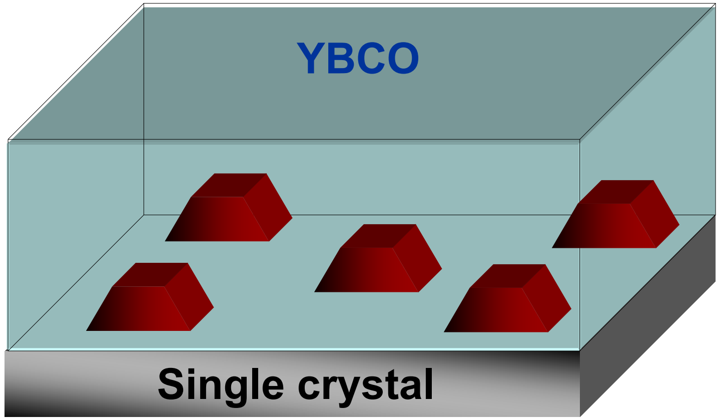

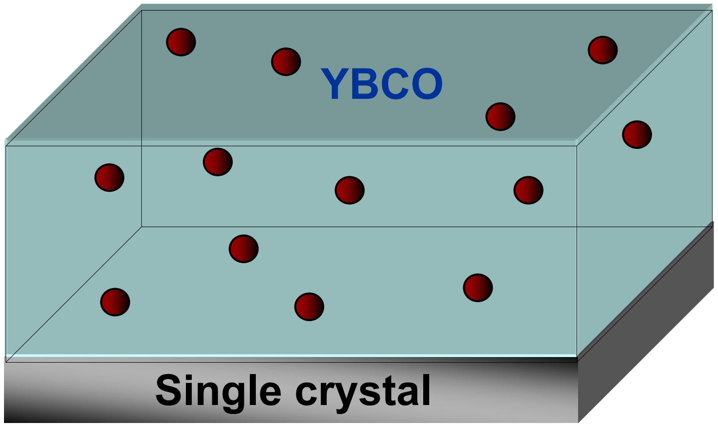

APS : Artifical Pinning Structures

Pinning of vortices by material defects

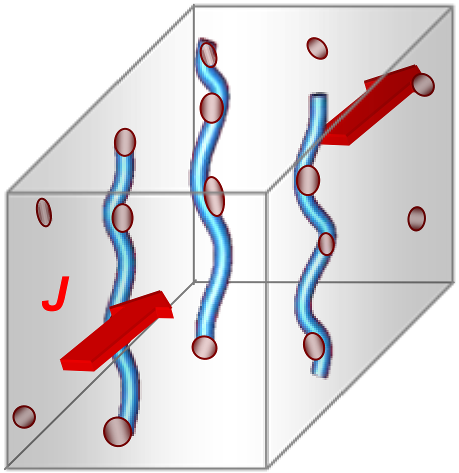

$F_L = J_c \times B = F_p \rightarrow v_{fl} = 0$

Current flow without dissipation

Generation of APS

HOW ?

… by nanostructuration

The methodology must be versatile, scalable and low cost

We choosed a chemical solution route

NEED of:

- Manipulation, control and tuning of APS
- Correlation of nanostructured films with J_c
- Knowledge on superposition of APS and natural defects
- More realistic theoretical pinning models considering complexity

Chemical Solution Deposition

… a versatile, scalable and low cost methodology for growth of nanostructured films

For YBCO films …

Spin-coating on a substrate

Metal-organic TFA solution

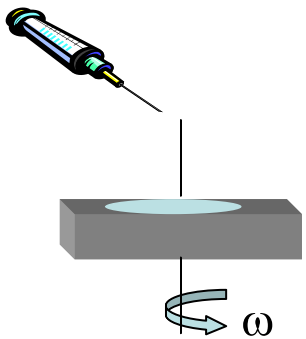

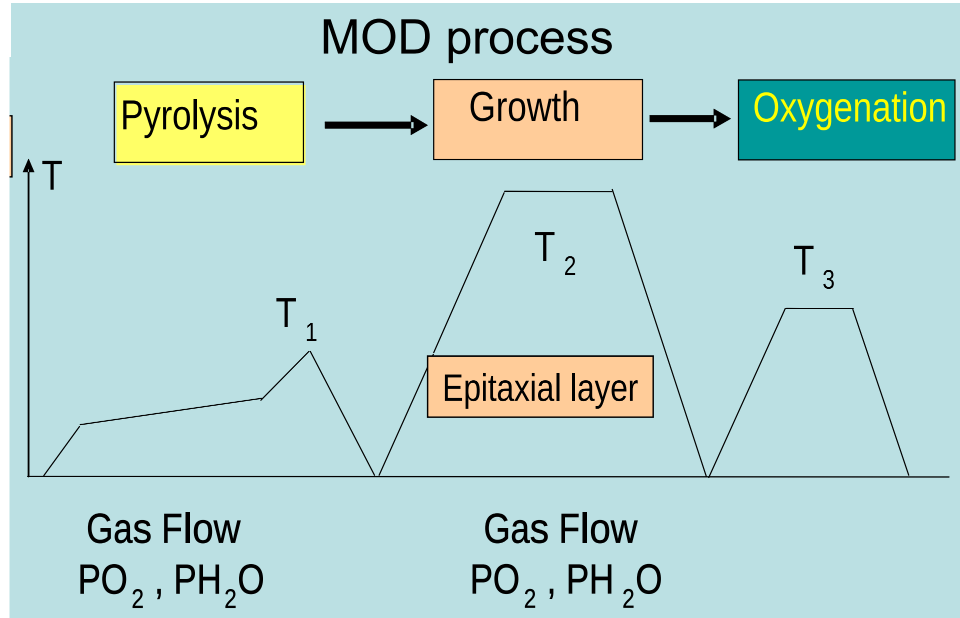

Coated conductors

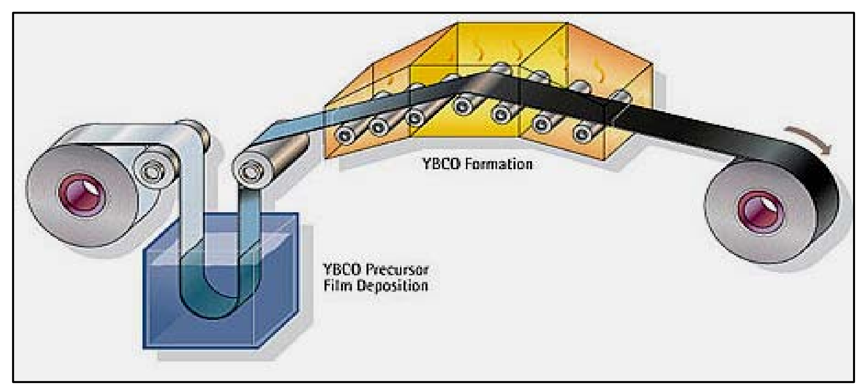

- **Low-cost methodology**
- **High production rate**
- **Scalable to large surfaces**
- **Versatile: nanostructuration**

Phase and growth control

Film quenched before growth

- Intermediate phases: a-Y_2O_3,$Y_2Cu_2O_5$ and CuO embedded in oxyfluorides (OF)
- YBCO nucleates exclusively at the interface: island to layer growth

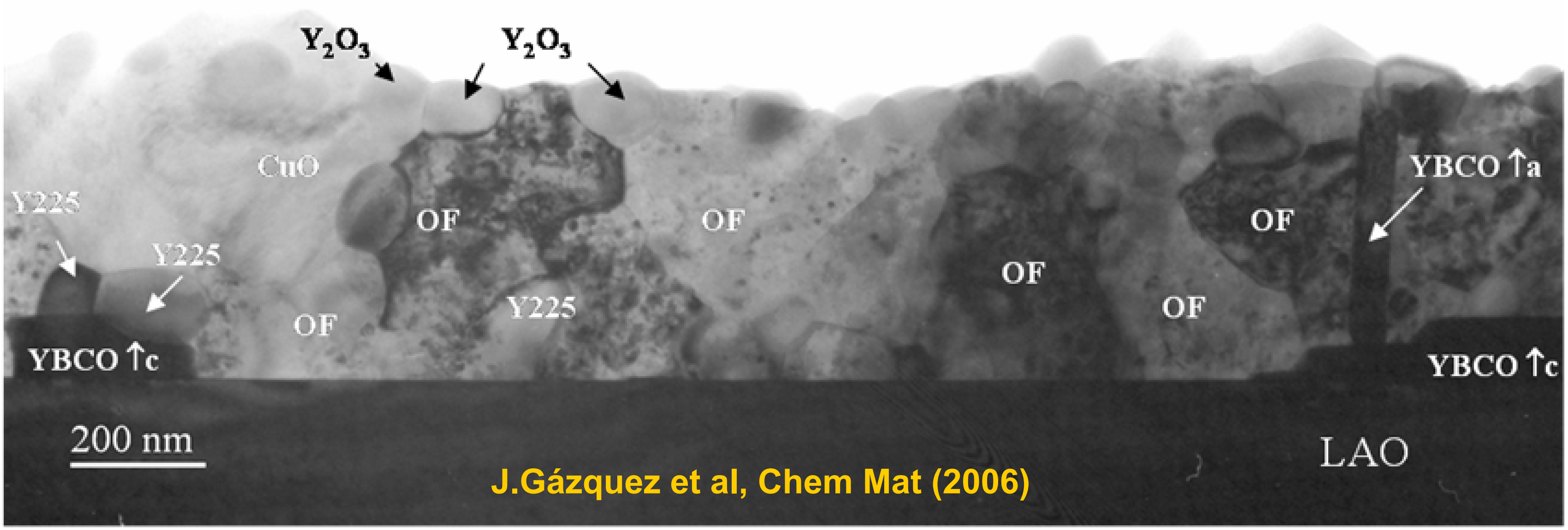

Y long and winding road: TFA-Y / $Ba_{1-x}Y_xF_2$ / a-Y_2O_3 / $Y_2Cu_2O_5$ / $Ba_{1-x}Y_x(F,O)_{2-y}$ / $YBa_2Cu_3O_7$

Multilayers: Epitaxy and cap layer planarity

$Ce_{1-x}[Gd(Zr)]_xO_{2-y}$

RHEED

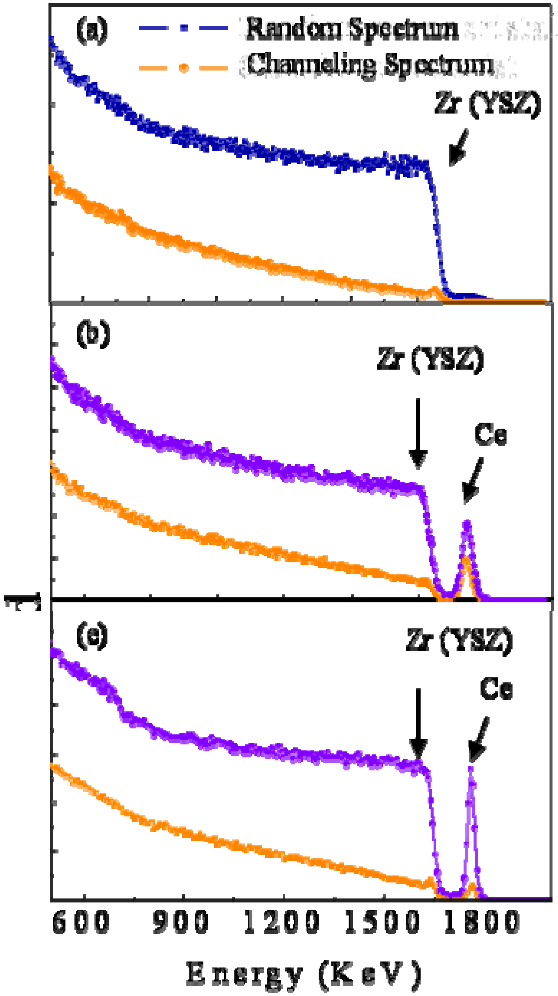

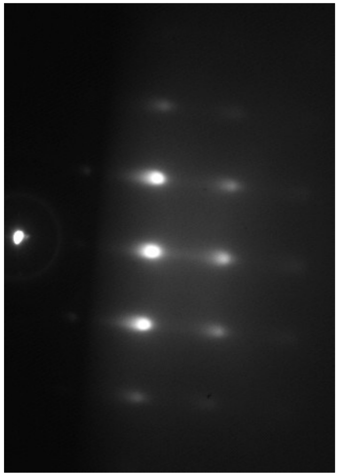

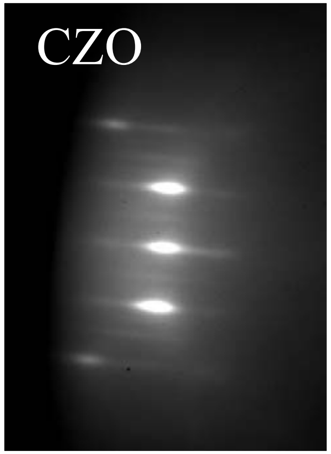

RBS channeling

χ_{min} = 12 % (CeO_2)

χ_{min} = 46 % (CZO)

High energy (00l) facets

AFM

rms: 3 nm

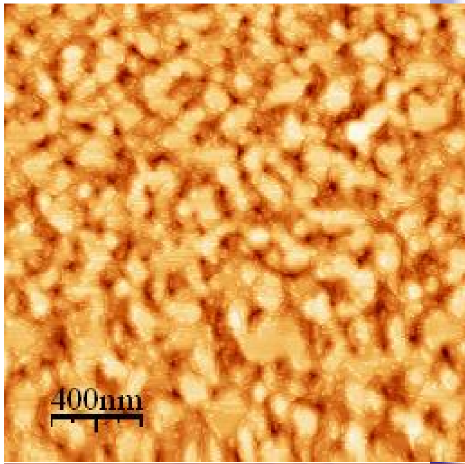

rms: 0.8nm

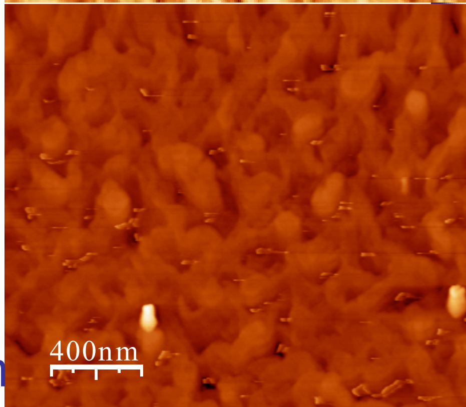

Growth of $^{TFA}YBCO$ on MOD CeO_2 cap layers

rms roughness is too rough

Surface planarity is more useful

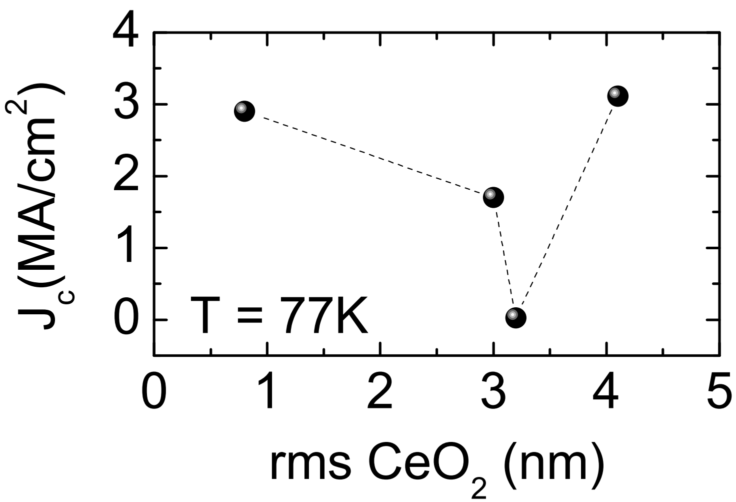

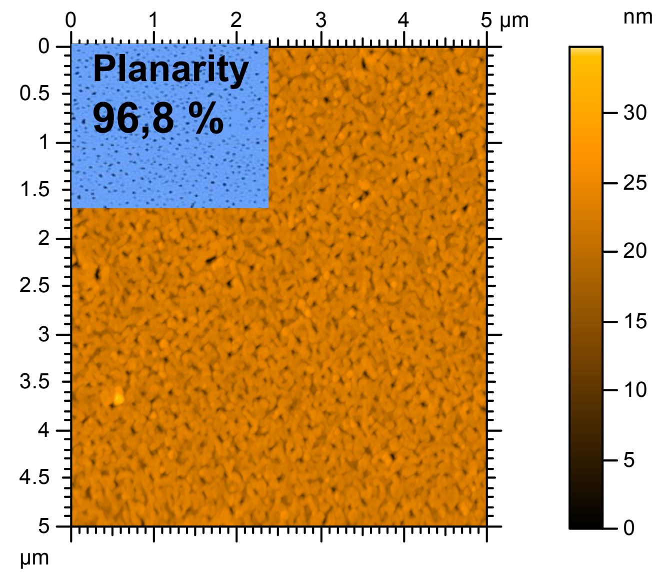

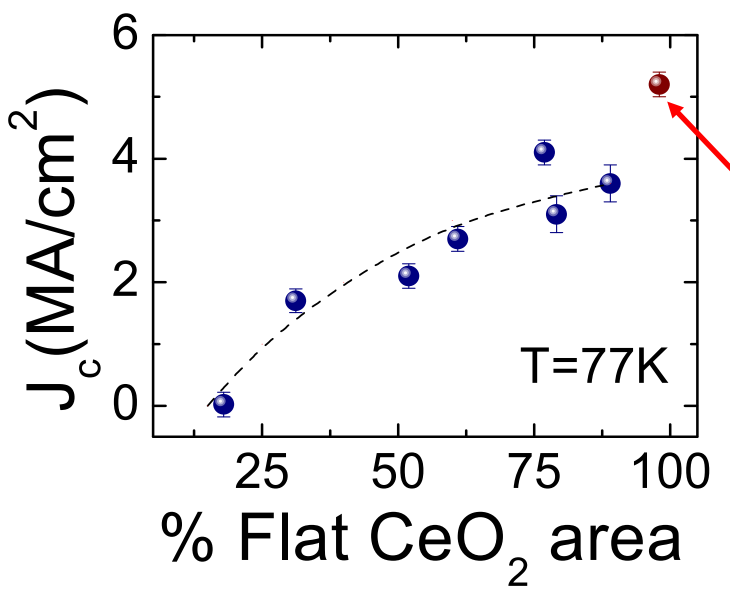

J_c (77K)= 5.2 MA/cm^2

Highest critical current $^{TFA}YBCO$ on MOD-CeO_2 cap layers

Growth of ^{TFA}YBCO on MOD-cap metallic substrates

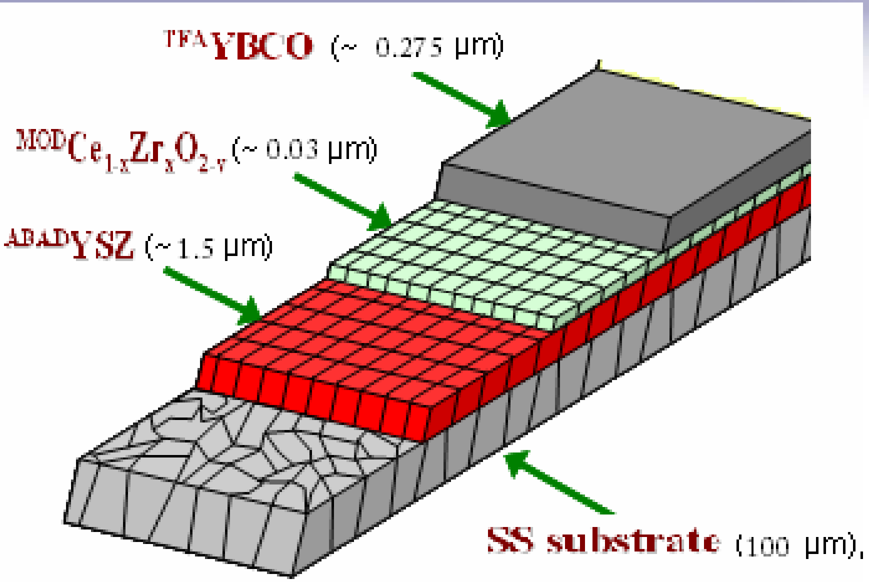

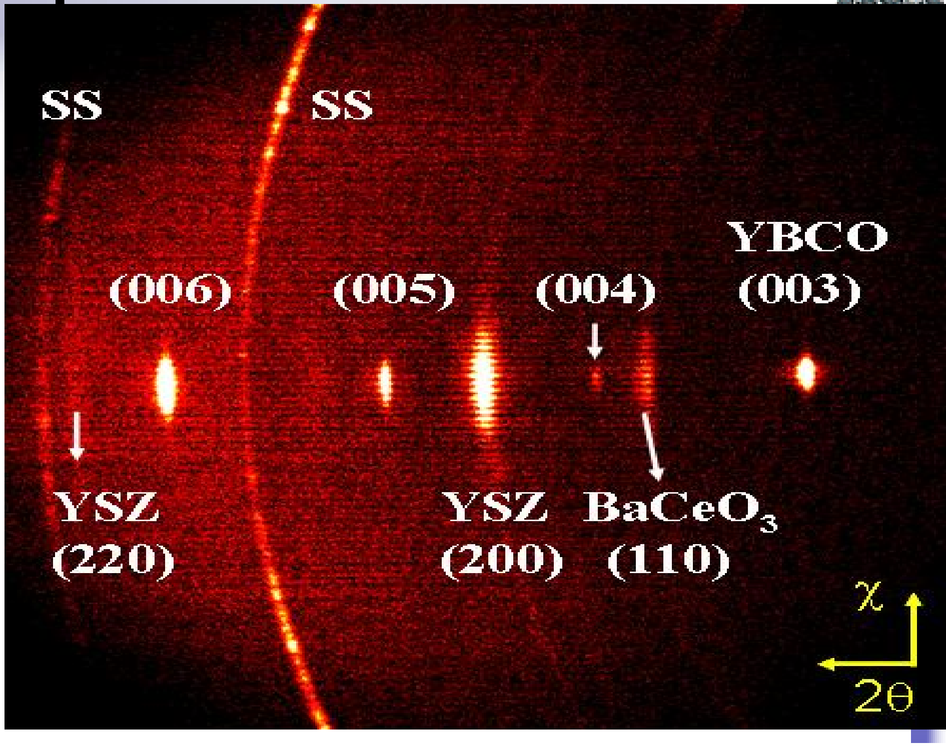

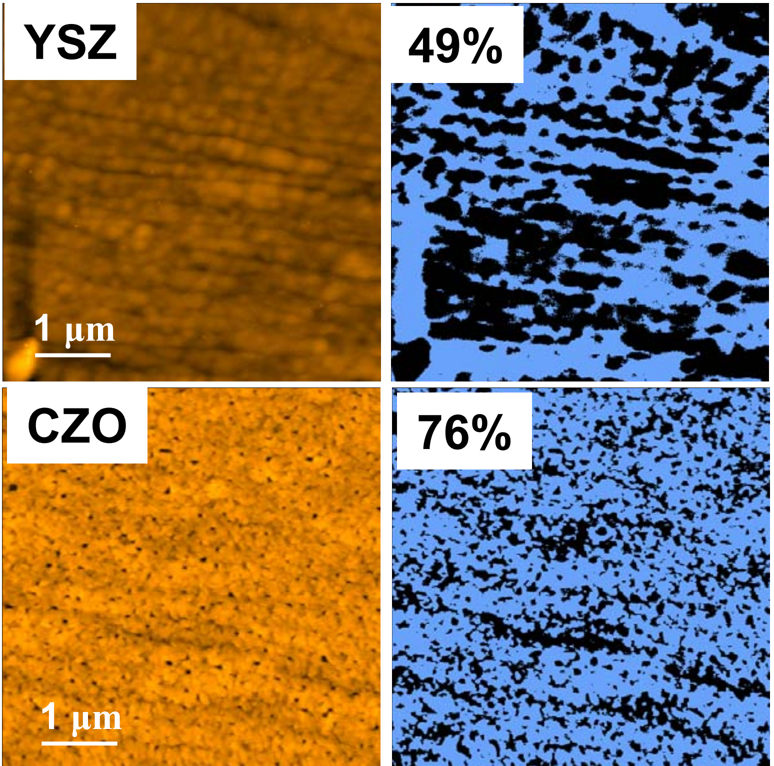

Polycrystalline substrate/epitaxial multilayer

$\Delta\phi$ (YBCO) =5º

$\Delta\phi$ (YSZ) =9.5º

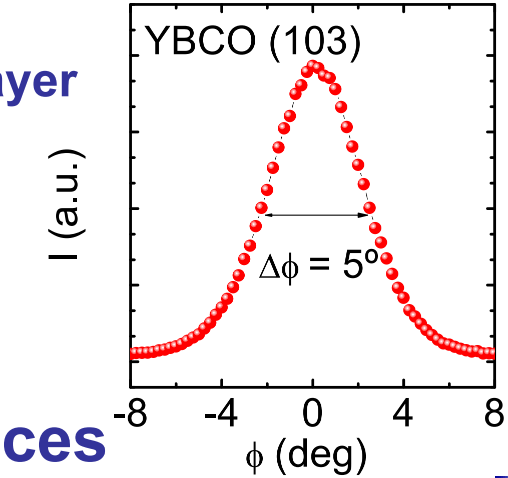

MOD planarization

High SC performances

J_c (77K)= 1.8 MA/cm^2

EHTS European High Temperature Superconductors
A member of Bruker Biospin

Vortex pinning in MOD-YBCO films

High quality epitaxial films
$J_c^{sf}(77K) \sim 4\ MA/cm^2$

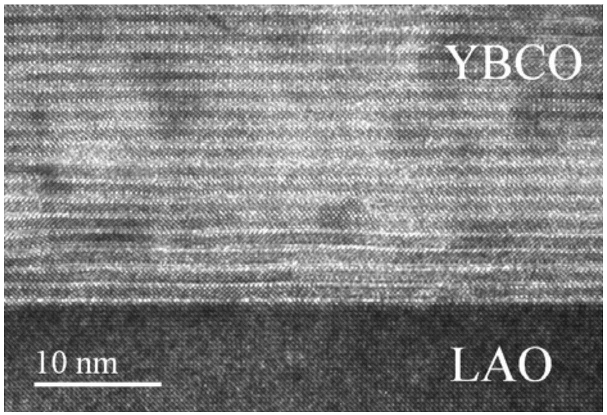

Island based nucleation and growth mode → a-b plane defects promotion

- Intergrowth
- Stacking faults
- in-plane partial dislocations

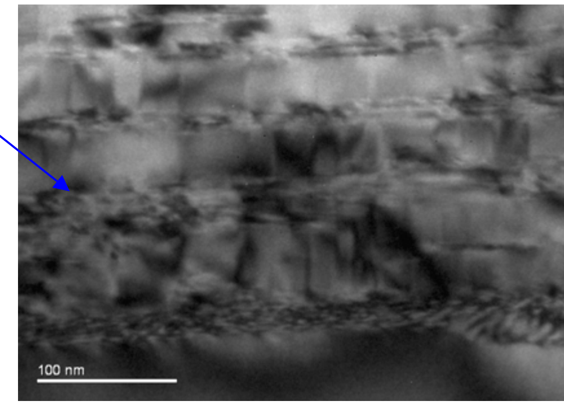

Critical current optimization → at high fields (1- 5T)

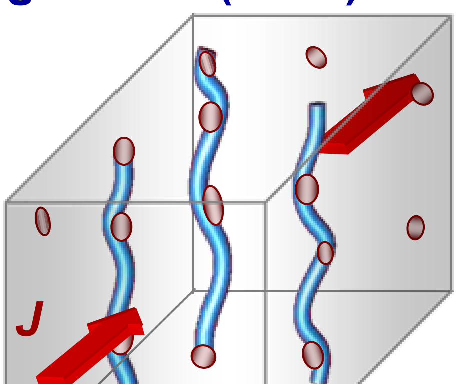

Correlation nanostructure and vortex pinning

Pinning defects of specific size and disposition

Point like defects

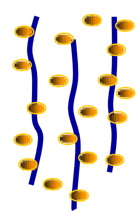

Linear defects

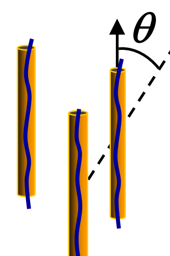

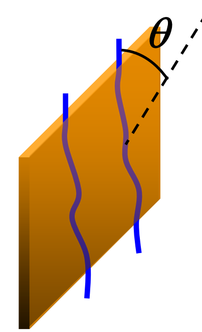

Planar defects

We need to identify and separate different vortex pinning contributions

Isotropic and anisotropic pinning defect contributions

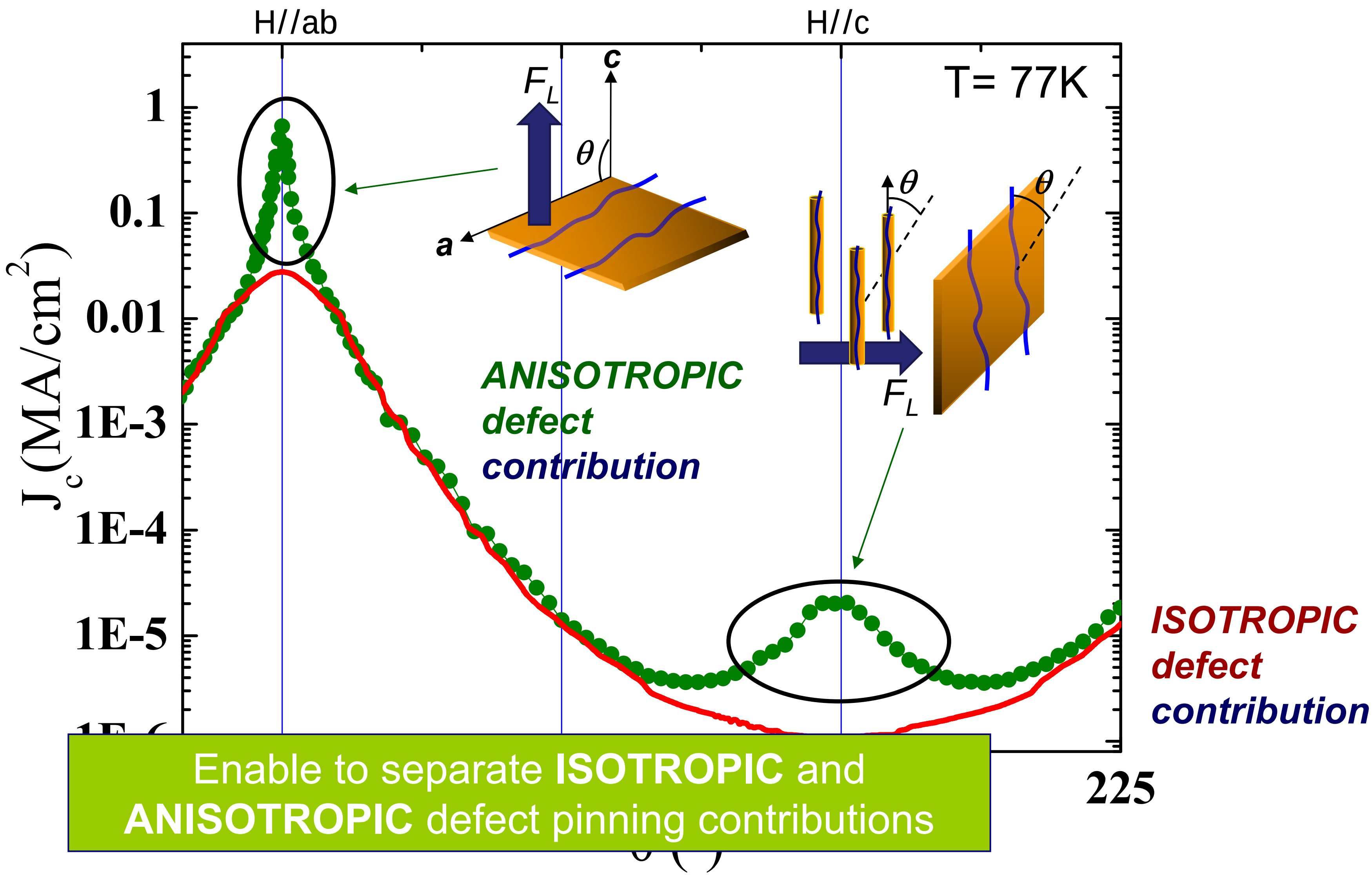

Enable to separate **ISOTROPIC** and **ANISOTROPIC** defect pinning contributions

MOD-YBCO, t ≈ 275 nm

J_c temperature dependence: Weak and strong pinning

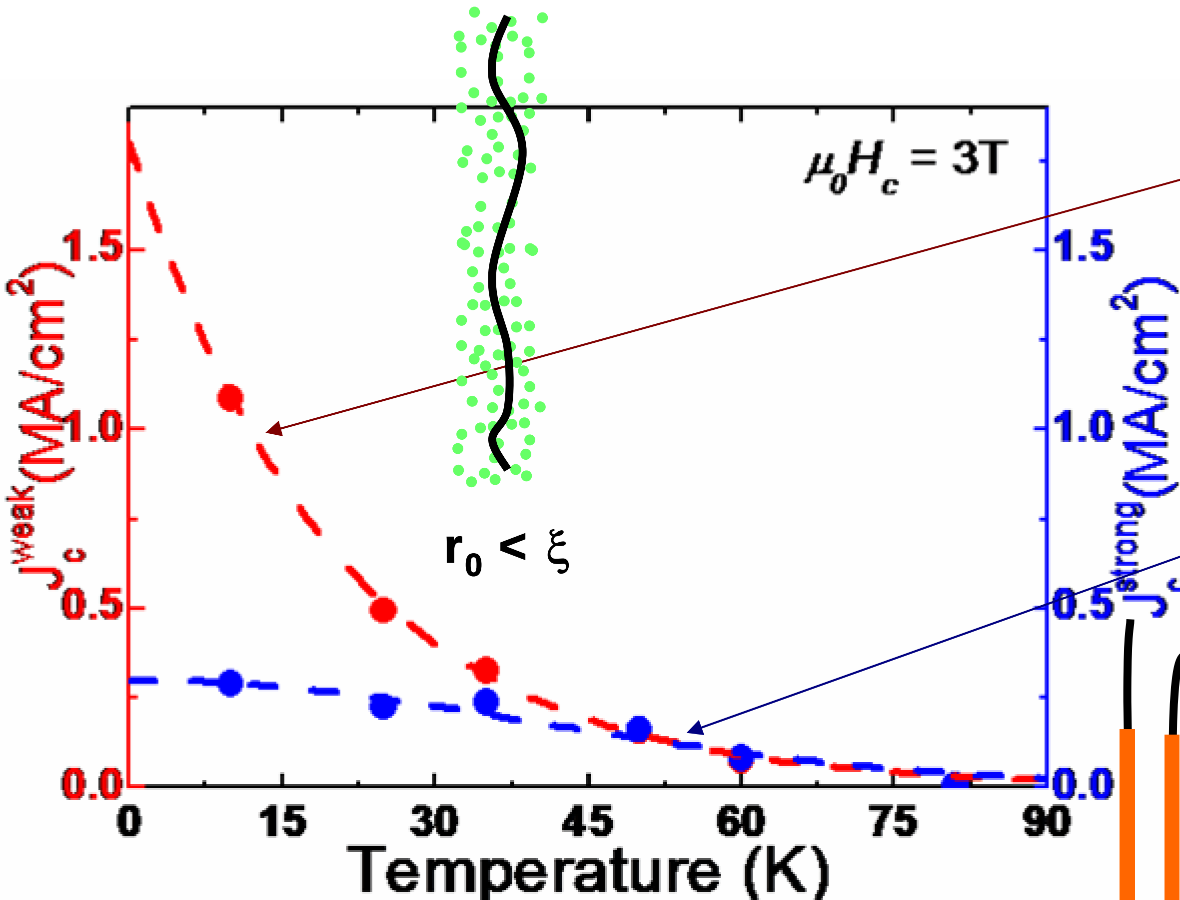

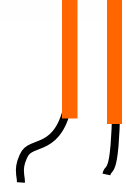

PLD-YBCO

Weak pinning

$$J_c(T) = J_{c0}^{wk} e^{-T/T_0}$$

*Blatter et al., Rev. Mod. Phys **66** (1994)*

Strong correlated pinning

$$J_c(T) = J_{c0}^{str} e^{-3(T/T^+)^2}$$

*Nelson et al, Phys. Rew. B **48** (1993)*

*J.Gutierrez et al., Appl. Phys. Lett. **90** (2007)*

Pinning regime diagrams in standard TFA films for H//c

Iso-wk contribution

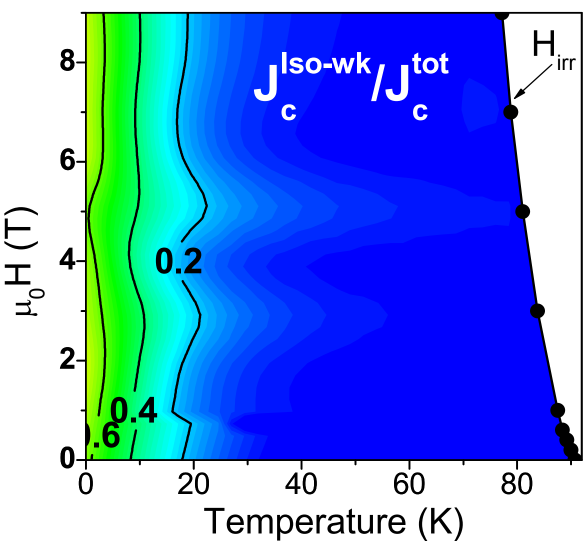

Iso-str contribution

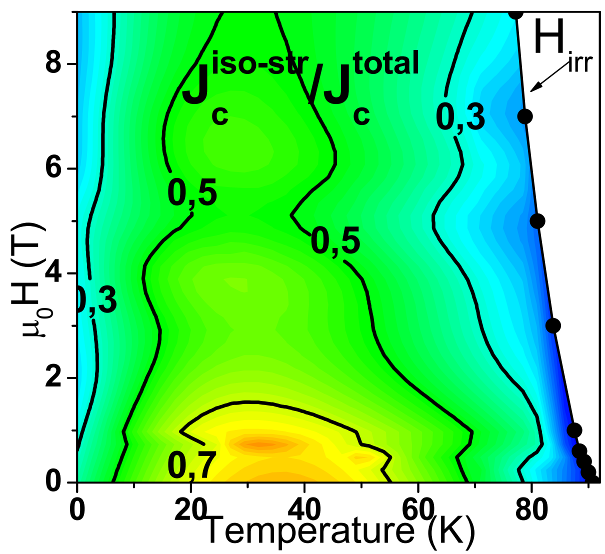

Aniso-str contribution

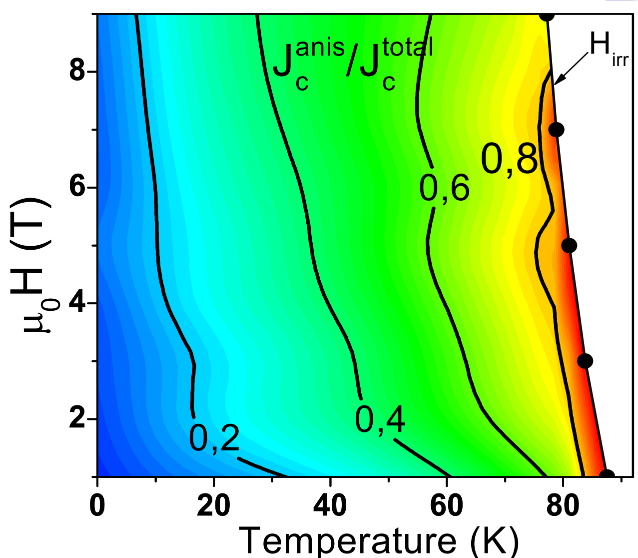

275 nm YBCO-TFA films

We have a tool to separate and quantify the three vortex pinning contributions

Weak-isotropic defects dominate at low T, **strong-isotropic** defects at intermediate T and **strong-anisotropic** defects at high T

T.Puig et al., SUST **21,** 034008 (2008)

Vortex pinning in nanostructured YBCO-TFA films

Interfacial nanostructured films:

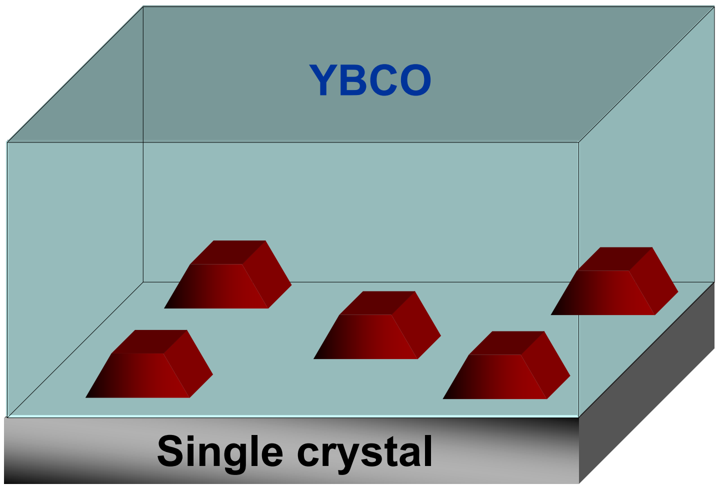

Nanocomposite films:

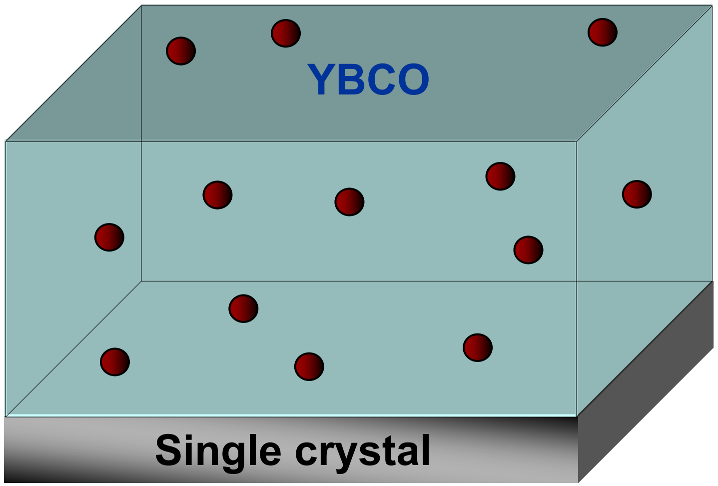

Approach:

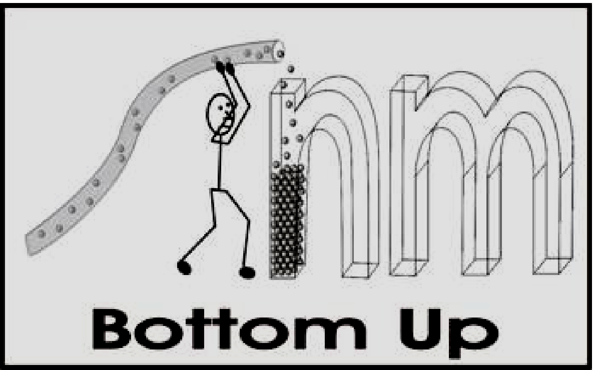

AIM: Identify and control pinning contributions induced in the different nanostructured YBCO films

Nanostructures: Chemical Solution Deposition

Metal-organic precursors → Spin-coating on a substrate → Thermal treatment

Pentadionates, acetates, propionates in acetic acid, isopropanol and/or propionic acid

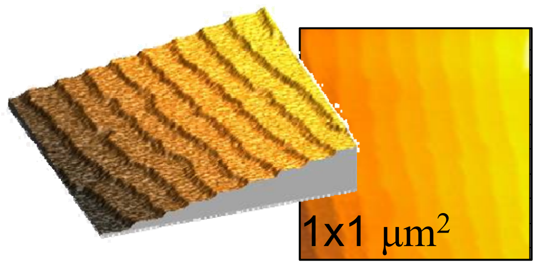

single crystal thermally treated

$600^oC \leq T \leq 1000^oC$

Atm: O_2, Ar-H_2

Use of very dilute solutions → **Tune of the equivalent deposited thickness through concentration**

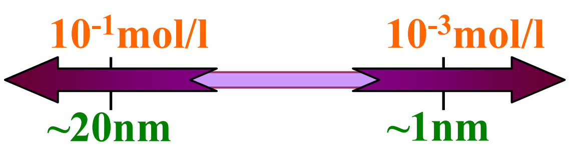

complete layer

Self-assembled nanoparticles

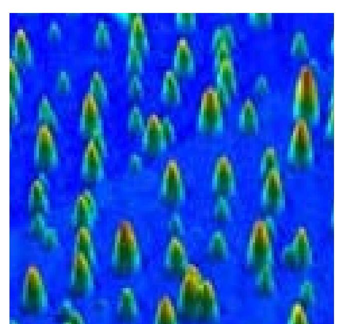

Surface energy
Interface energy
Elastic relaxation energy

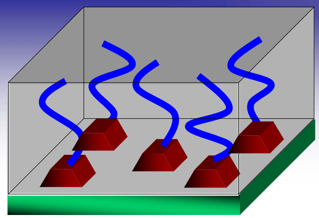

Interfacial self-assembled nano-structured films

Self-assembled nanostructures grown from chemical methods

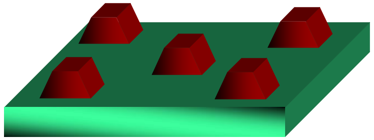

- **Strain induced self-assembled $Ce_{0.9}Gd_{0.1}O_{2-y}$ nanowalls**

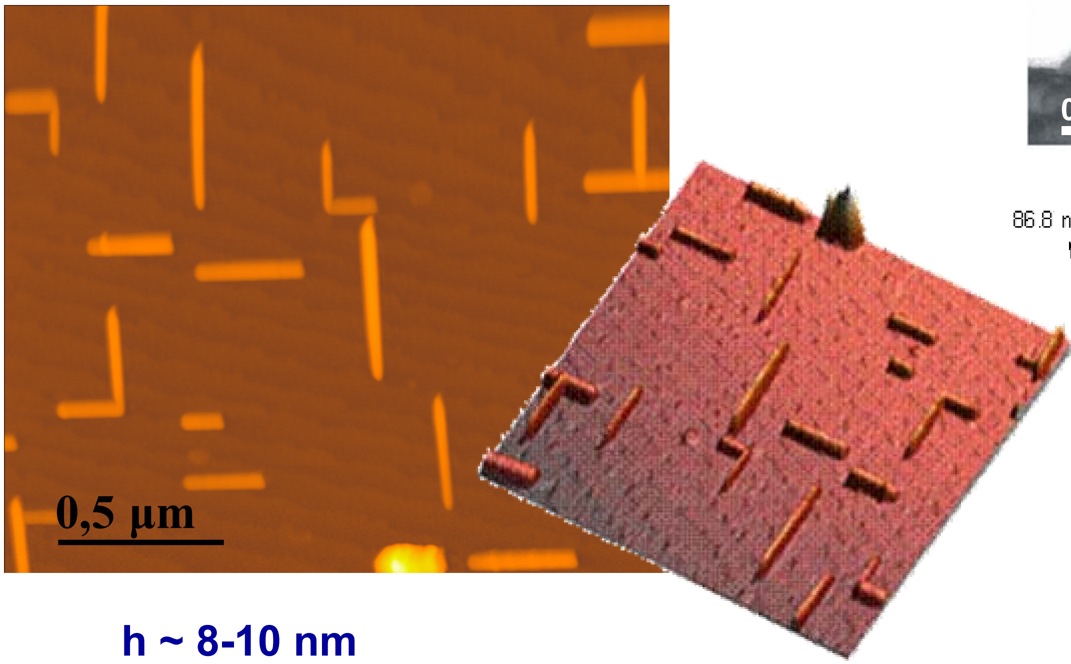

h ~ 8-10 nm

M. Gibert et al., Adv. Mat. 19, 3937 (2007)

- **Spontaneous nucleation of $(La,Sr)O_X$ nanoislands on LSMO**

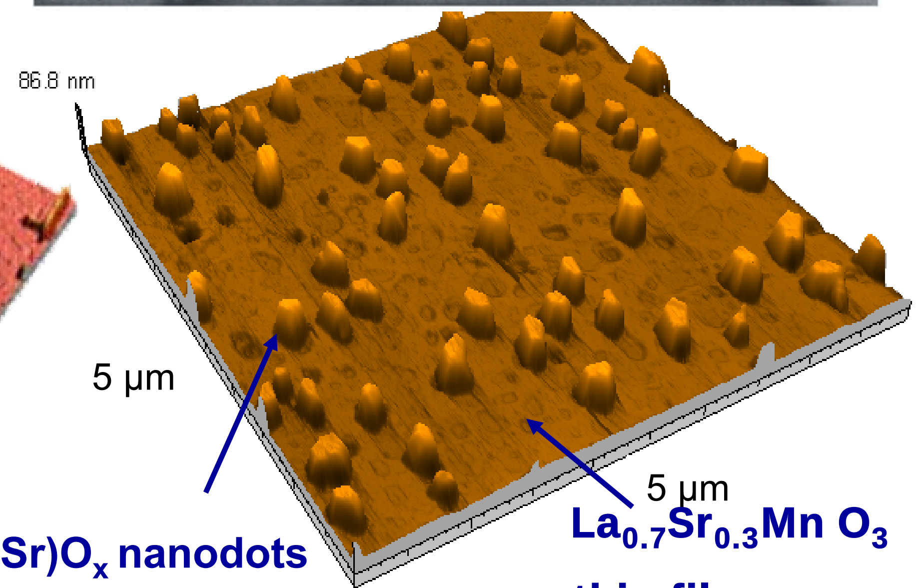

$(La,Sr)O_x$ nanodots
h ~ 50 nm

$La_{0.7}Sr_{0.3}Mn\,O_3$ thin film

C. Moreno et al. Adv.Func.Mat. (2009)

Nanodot and nanowires of $Ce_{0.9}Gd_{0.1}O_{2-y}$

Growth atmosphere: fine selection of interface energy

Isotropic islands

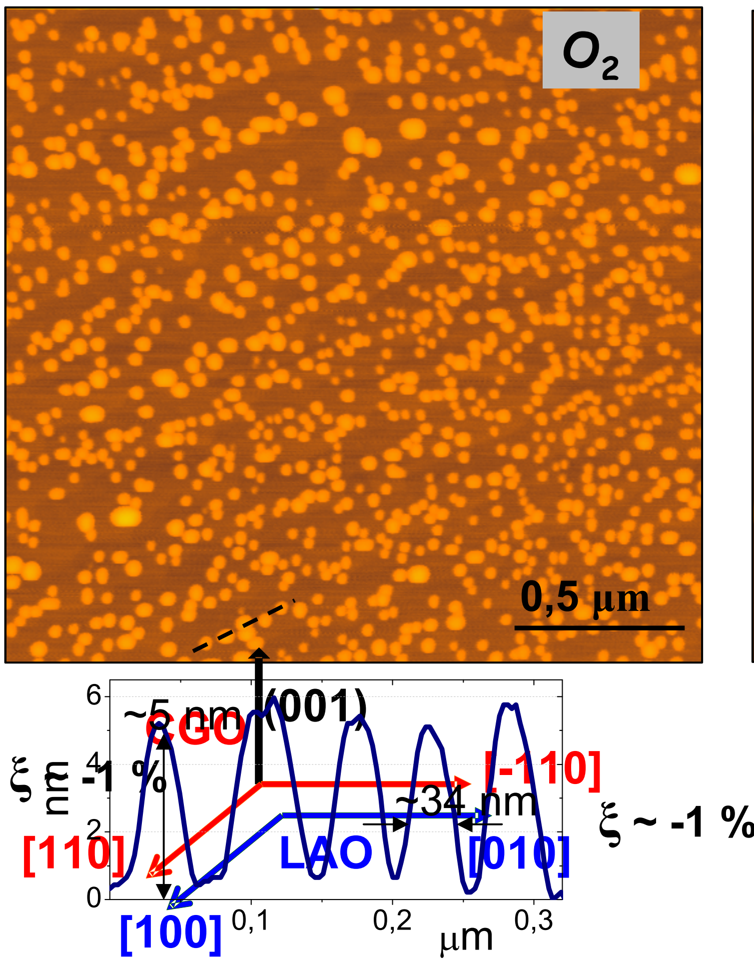

Highly anisotropic islands

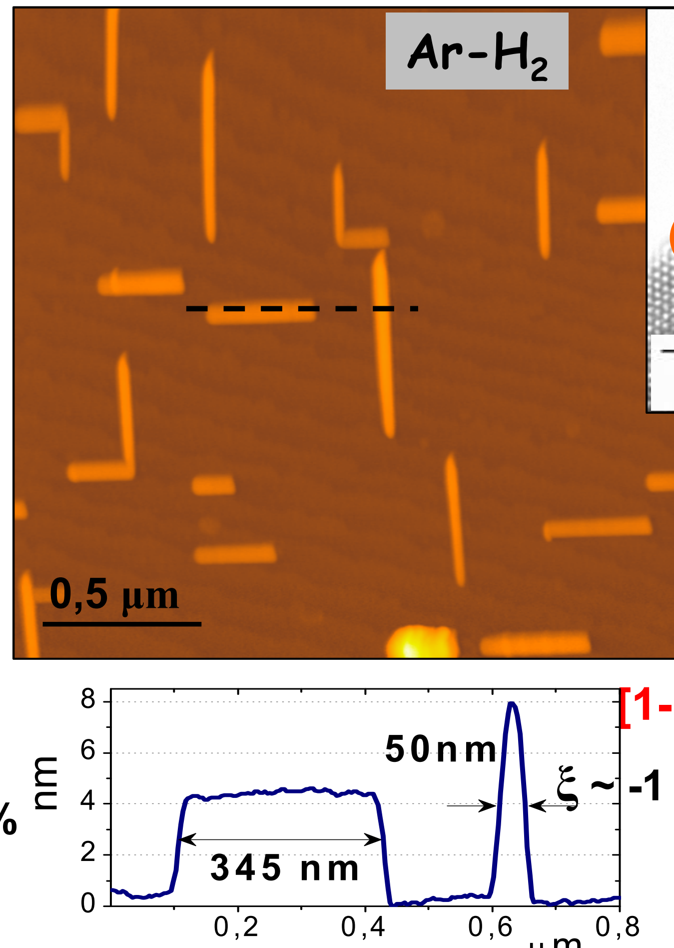

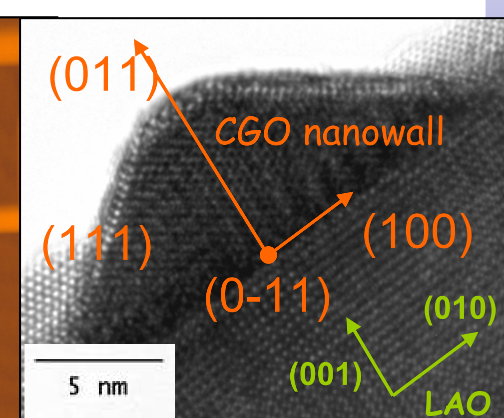

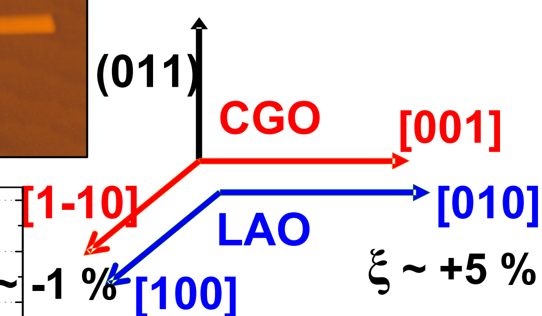

Interfacial oxide nanostructured films: Anisotropy of $J_c(\theta)$

Reduced anisotropic contribution for H//ab

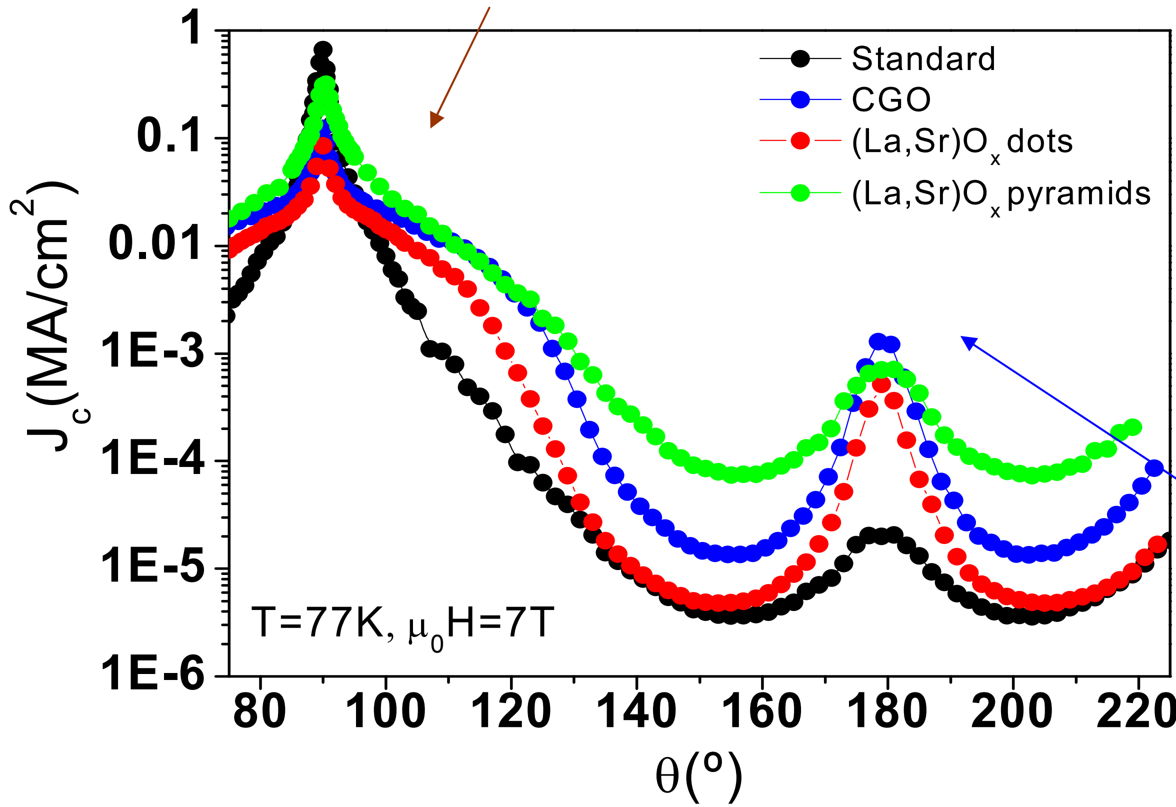

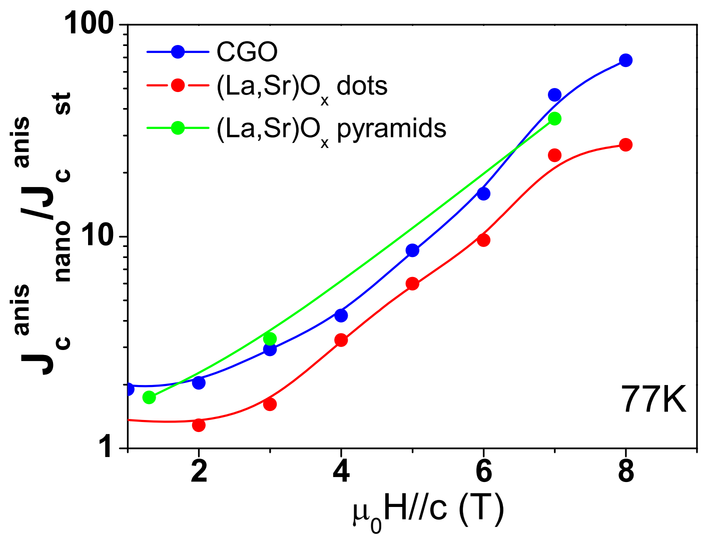

c-axis anisotropic contribution is strongly increased

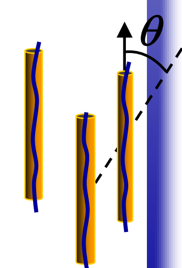

Similar behavior obtained for all the different architectures → defects along the c-axis induced in the YBCO matrix by the interfacial particles

J. Gutierrez et al., APL (2009)

Interfacial oxide nanostructured films: thickness dependence

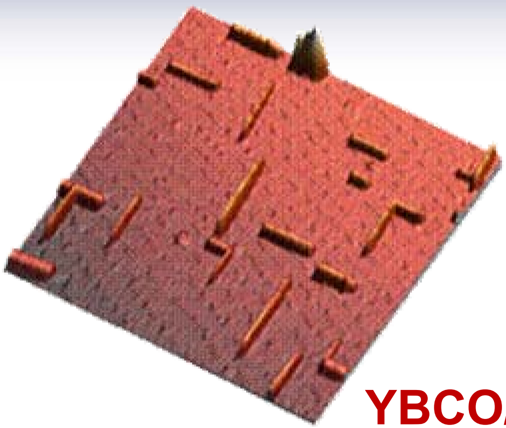

YBCO/$Ce_{0.9}Gd_{0.1}O_{2-y}$ nanowalls

4 tracks (20μm*100 μm) defined by lithography:

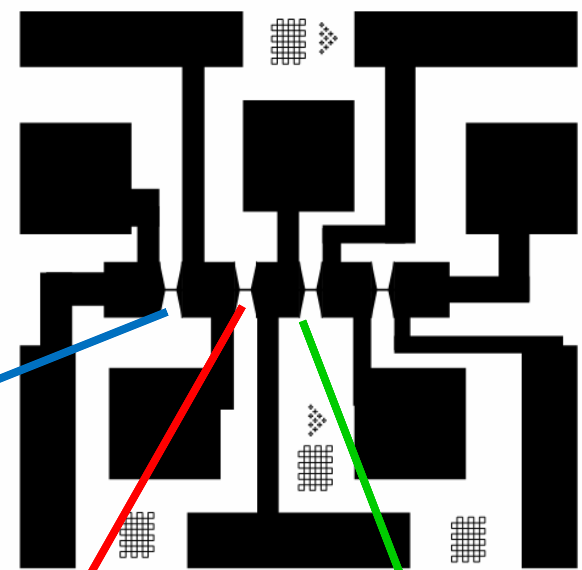

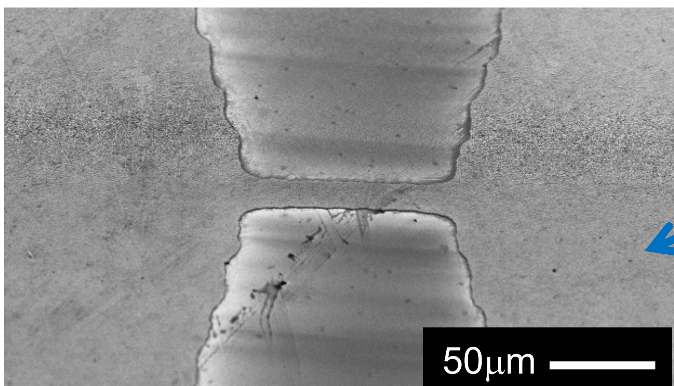

Track 1: full thickness 250nm

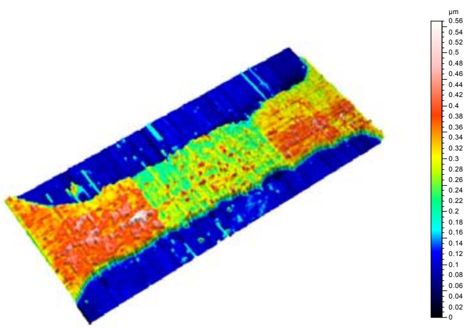

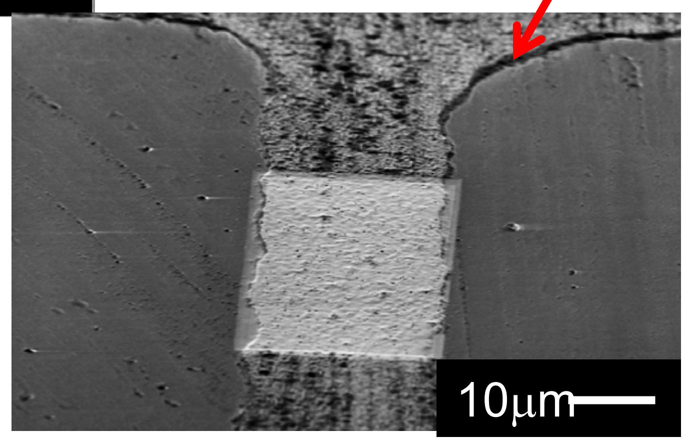

Track 2: FIB milling down to 175 nm

Track 3: FIB milling down to 130nm

Angular measurements

$\mu_0 H$ = 5T, T= 50K

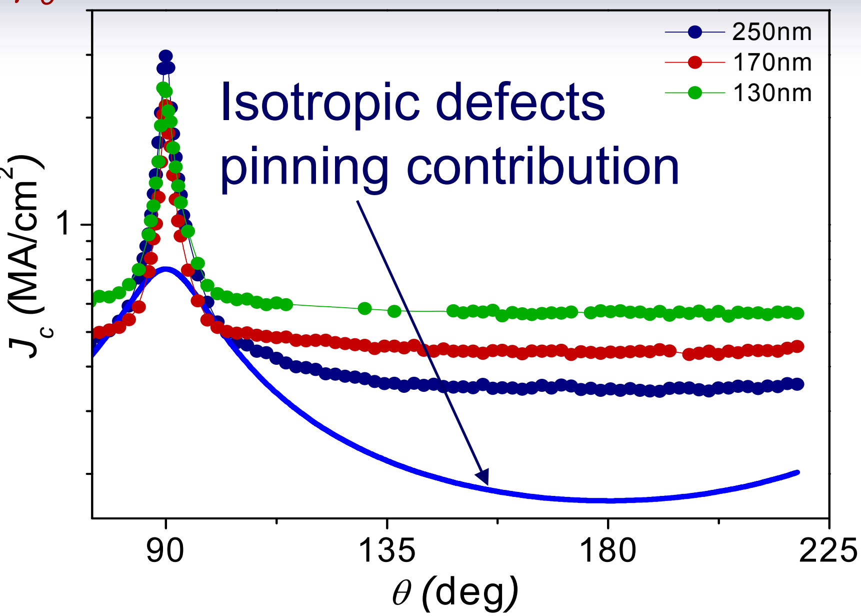

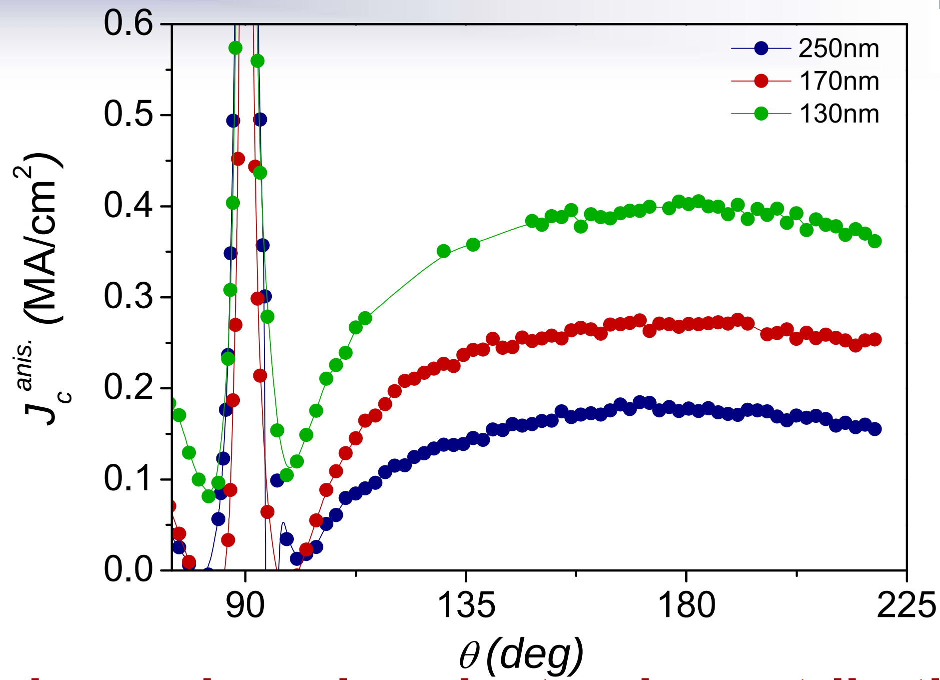

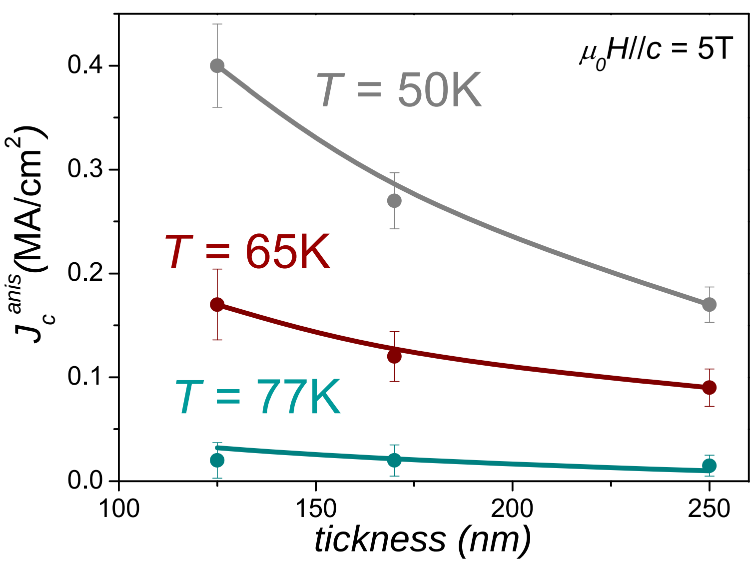

Enhanced c-axis anisotropic contribution as thickness decreases

Pinning associated to defects induced by interfacial nano-particles is enhanced by reducing the YBCO thickness → Higher density of defects generated near the nano-structures

In-situ YBCO^{TFA}-BZO nanocomposites

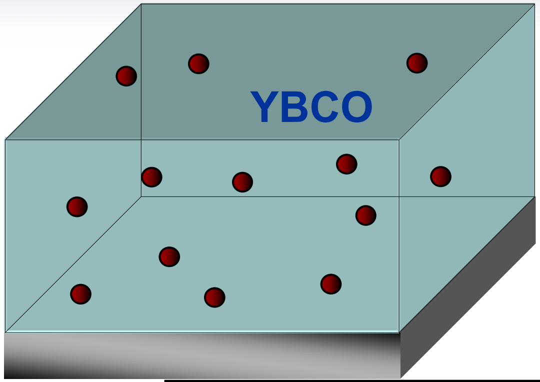

Modification of the (Y,Ba,Cu) precursor solution by addition of Ba and Zr salts: $BaZrO_3$ nanodots randomly embedded

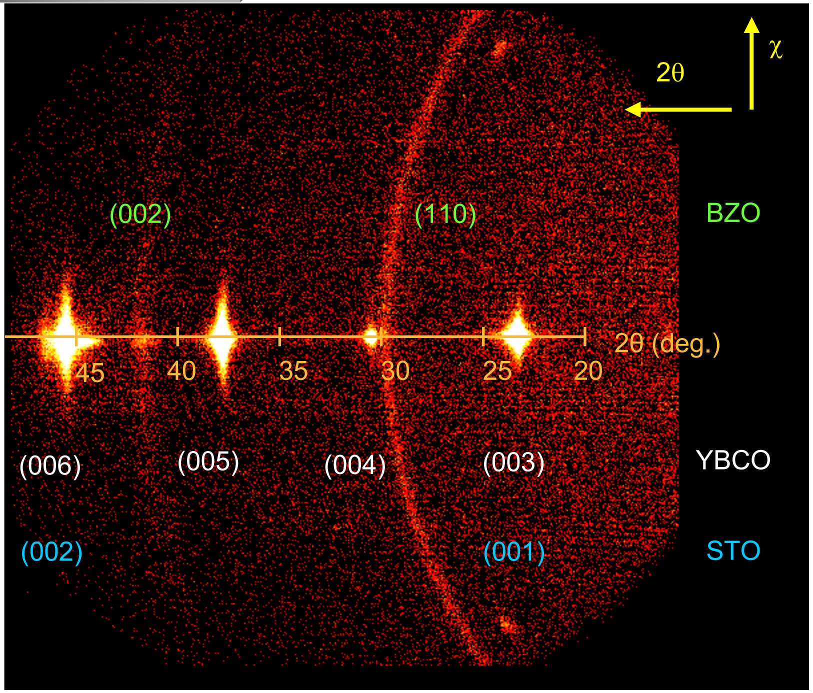

Film thickness= 200 (20) nm

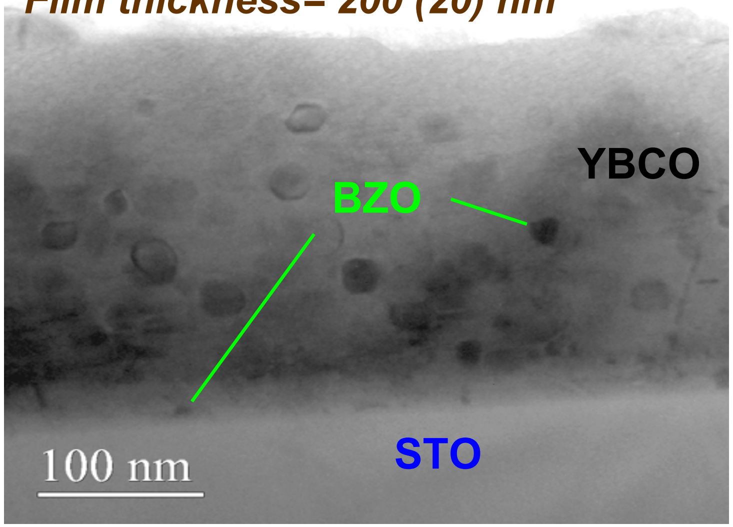

- BZO nanodots size : 10-20 nm

Two populations of BZO coexist

- Epitaxial
- Non epitaxial

J. Gutiérrez, A. Llordés et al., *Nature Materials* 6, 367 (2007)

YBCO^{TFA}-BZO nanocomposites

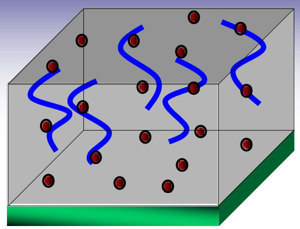

Modification of the (Y,Ba,Cu)TFA anhydrous precursor solution by addition of Ba and Zr salts

Film thickness= 200 (20) nm

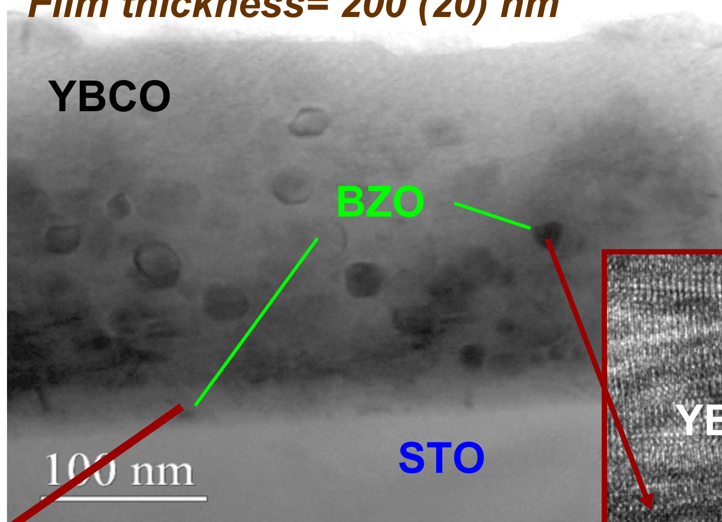

Interfacial nanodots

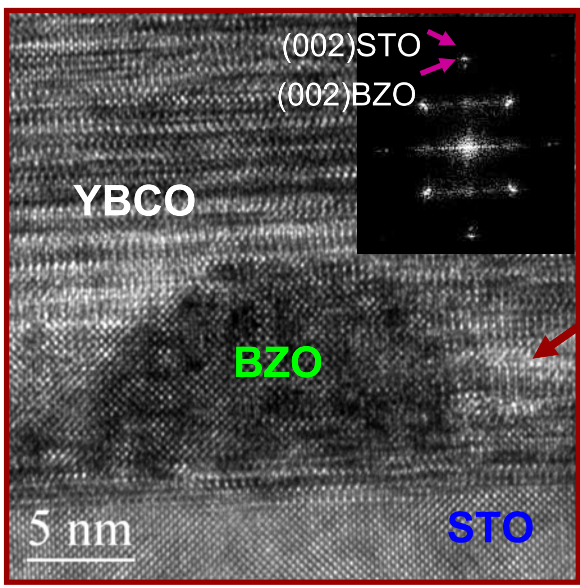

cube on cube epitaxial relationship with YBCO matrix

Bulk nanodots

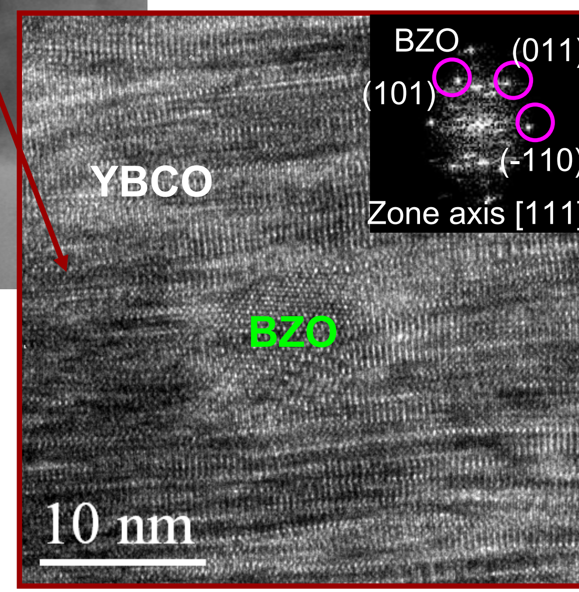

Randomly oriented (non-coherent with the matrix)

J. Gutiérrez, A. Llordés et al., *Nature Materials* 6, 367 (2007)

In-situ $YBCO^{TFA}$-Y_2O_3 nanocomposite

Epitaxial Y_2O_3 at the substrate interface and in the bulk

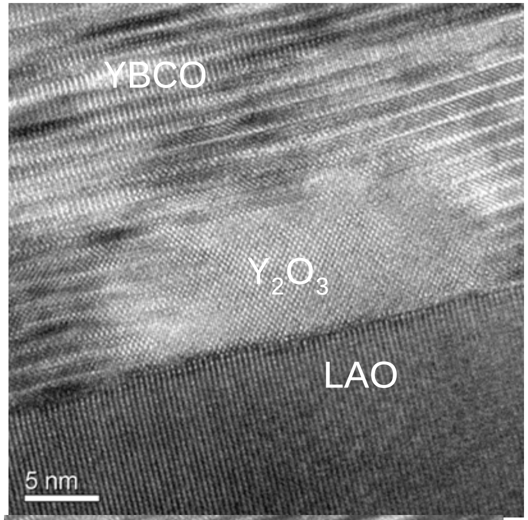

ε=-2.7 %

J_c(1T, 77K)=0.5 MA/cm^2 for 20 %mol

J_c(1T, 77K)=0.3 MA/cm^2 for 10 %mol

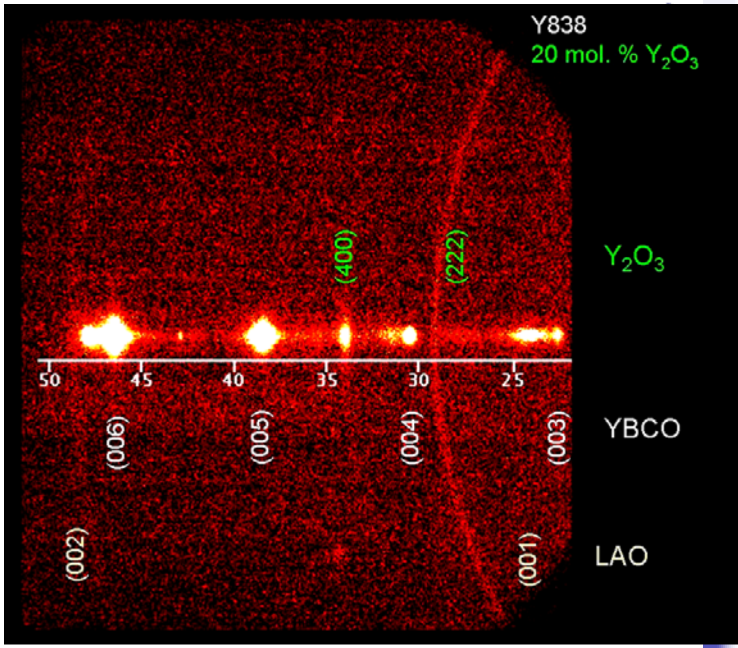

Y_2O_3 polycrystalline fraction is also present...BUT not identified by TEM

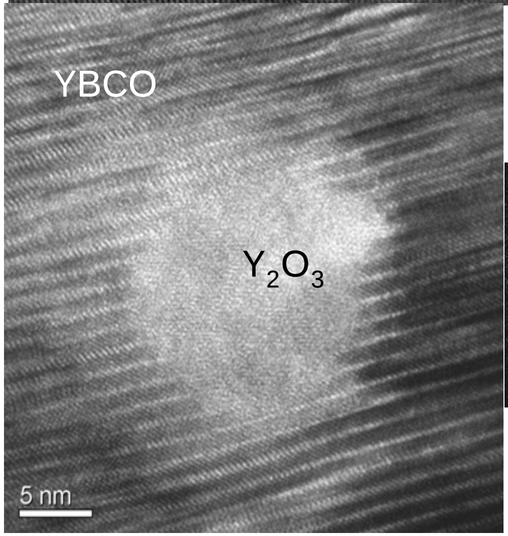

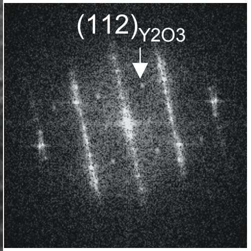

Average size Y_2O_3: 20-25nm

(001)Y_2O_3 // (001)YBCO
[110]Y_2O_3 // [100]YBCO

Need of quantification of non-coherent (or random) fraction

Interfaces in nanocomposites

- Can be divided, on the basis of their lattice matching, into three classes

↑ Interfacial energy

Coherent

γ **(coherent)=** γ_{ch}

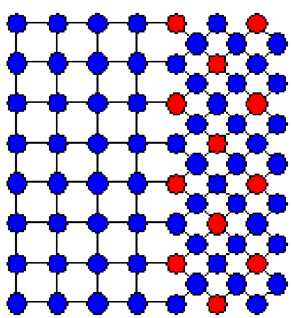

Perfect lattice matching at the interface plane

Semi-coherent

γ **(semi-coherent)=** $\gamma_{ch} + \gamma_{st}$

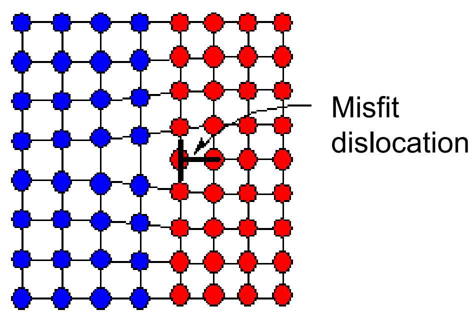

Lattice matching with strain relaxation

$$\boxed{\delta = (d_A - d_B)/\, d_A}$$

Incoherent

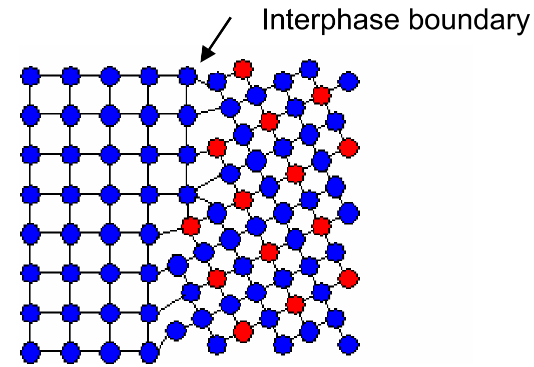

NO lattice matching

NO orientation relationship

Disordered structure

↓

Very little is known about the detailed structure

Epitaxial interfaces

Based on an orientation relationship which is specified crystallographically in terms of a pair of planes and directions: $\{hkl\}_A // \{hkl\}_B$ with $\langle uvw \rangle_A // \langle uvw \rangle_B$

Analogy interphase-grain boundaries

Interphase boundary

Interphase boundary

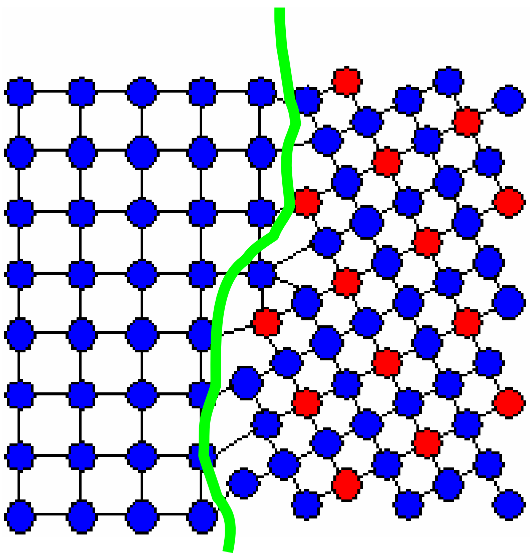

High interfacial energy

Nano-structural defects formation

- Stacking faults
- Chemical heterogeneities
- Twinning
- Dislocations
- Point defects
- Microstresses

Lattice strain (XRD)

High angle grain boundary

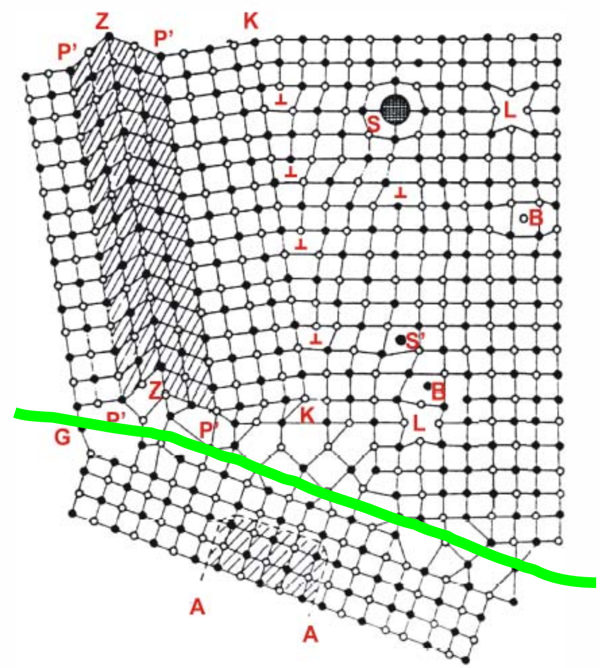

Enhanced pinning properties in SC nanocomposites are related to random Np

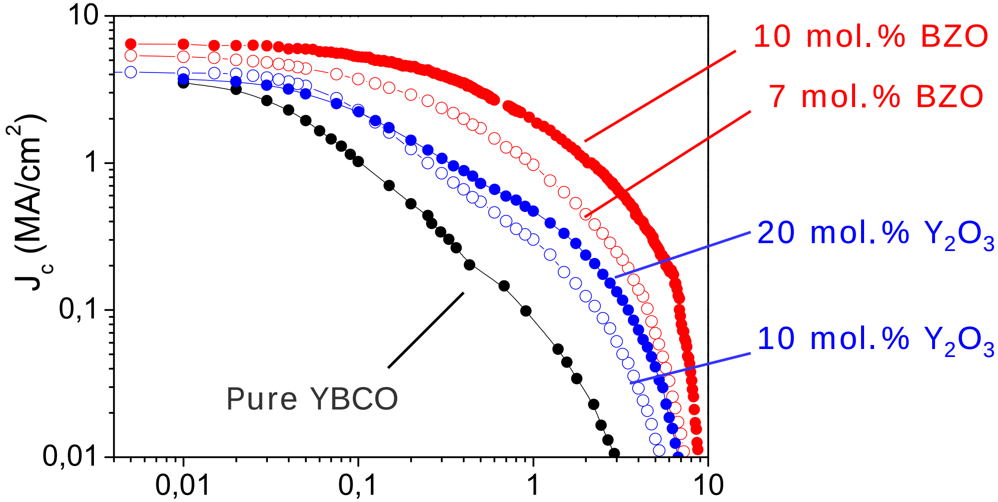

The strained microstructure is very effective to increase J_c at high magnetic fields (vortex pinning)

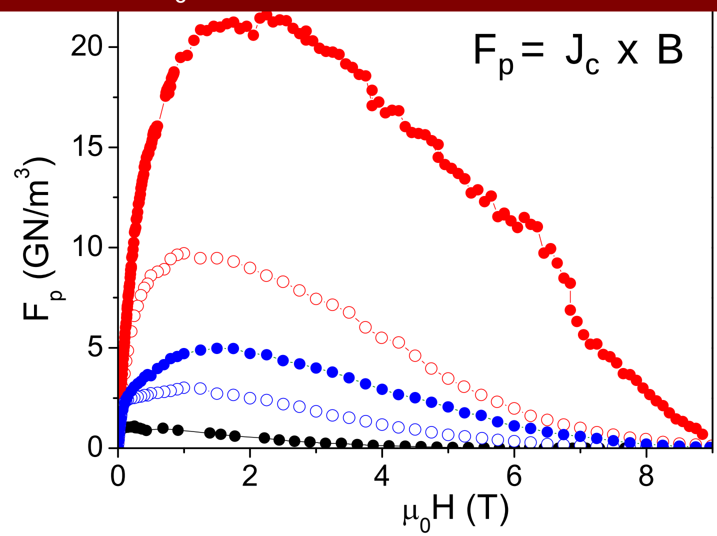

Maximum pinning force is controlled by random Np

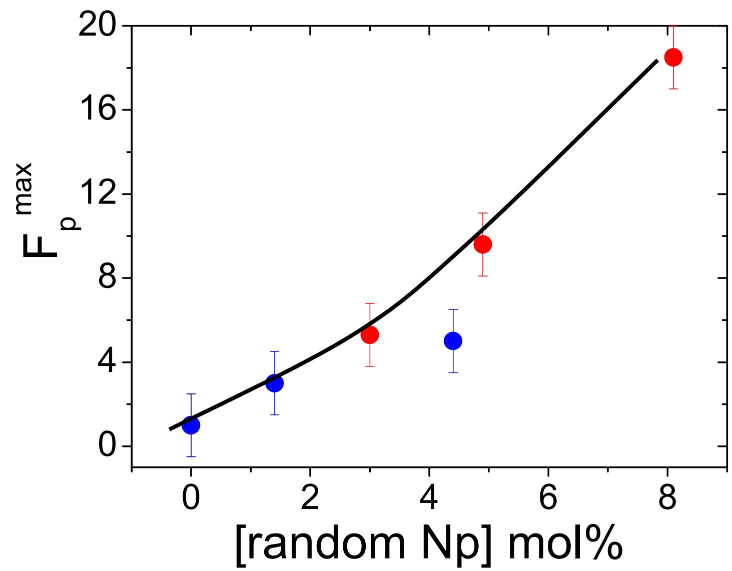

Isotropic microstrain plays an important role in vortex pinning propeties

$J_c(\theta)$ anisotropy is reduced in the nanocomposites

Vortex pinning is controlled by isotropic defects

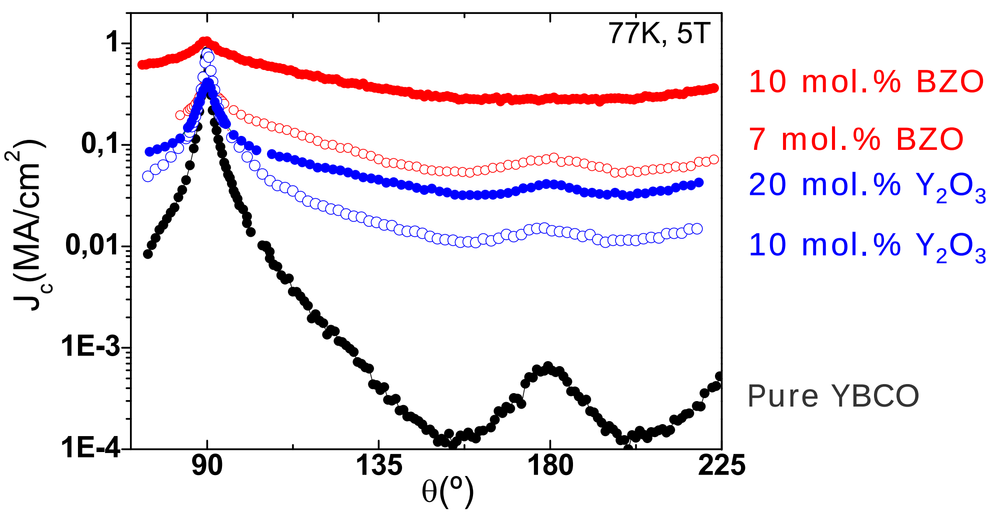

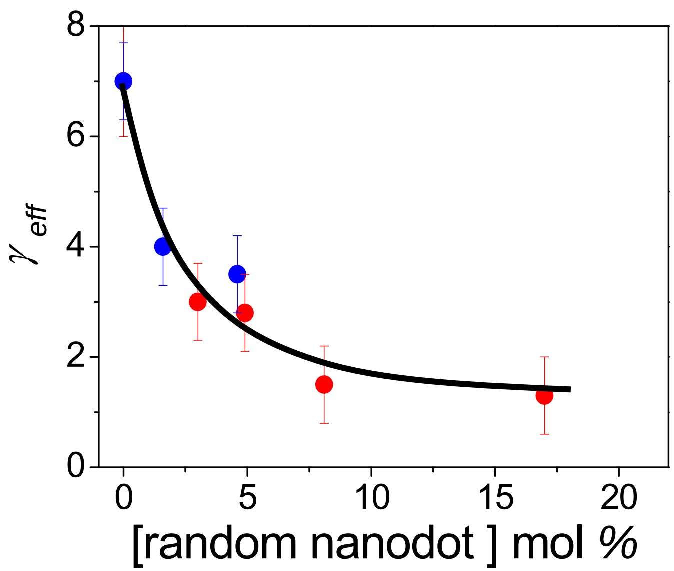

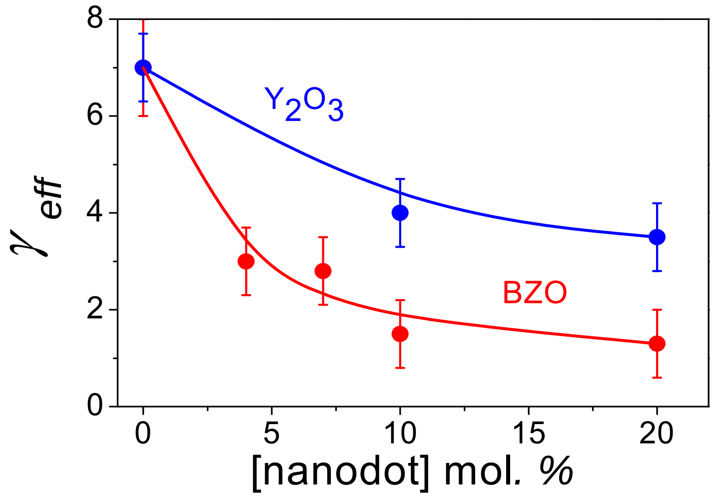

Random nanodots (isotropic microstrain) also control the effective anisotropy (γ_{eff})

Pinning regime diagrams

Iso-wk contribution

Iso-str contribution

Aniso-str contribution

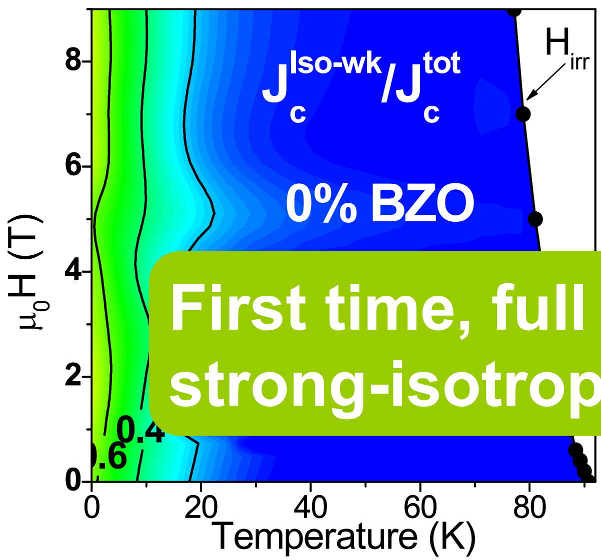

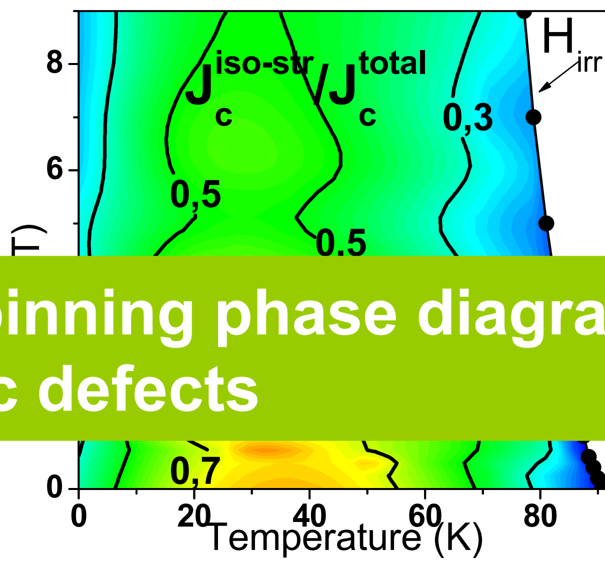

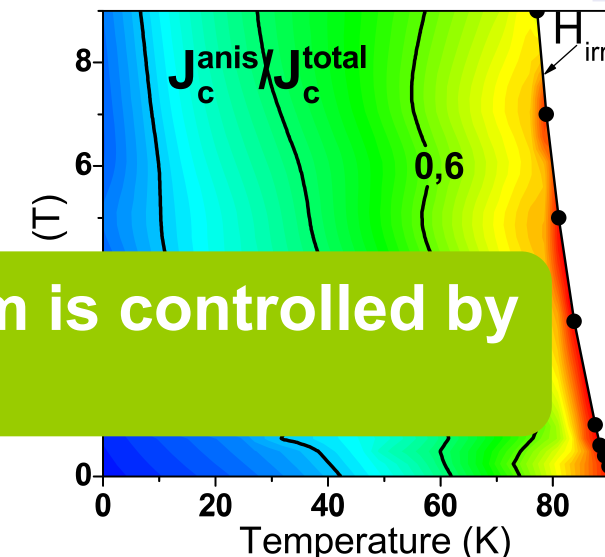

First time, full pinning phase diagram is controlled by strong-isotropic defects

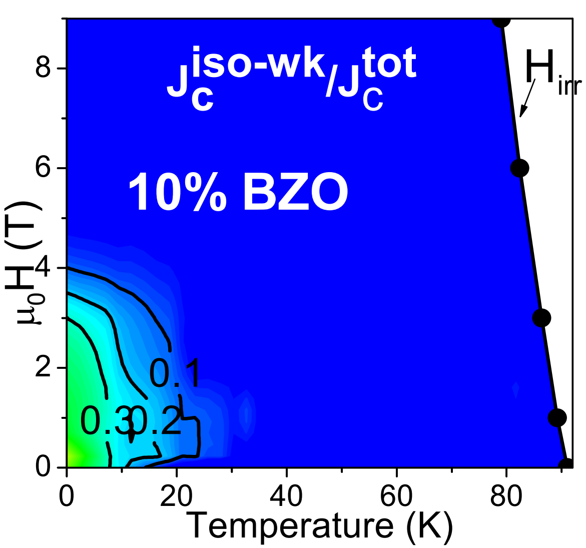

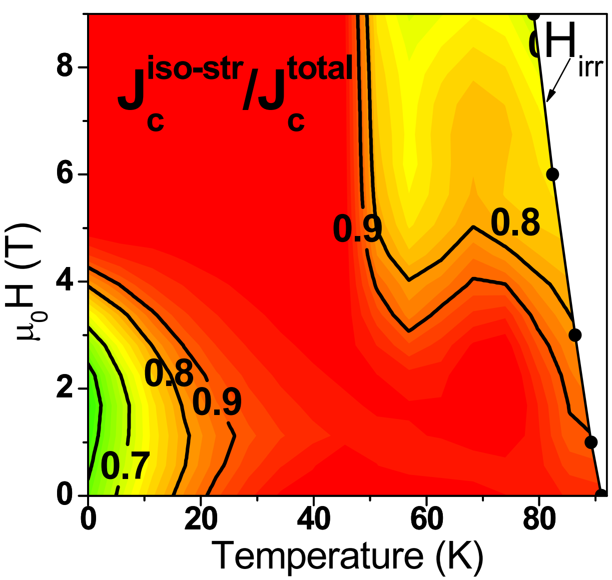

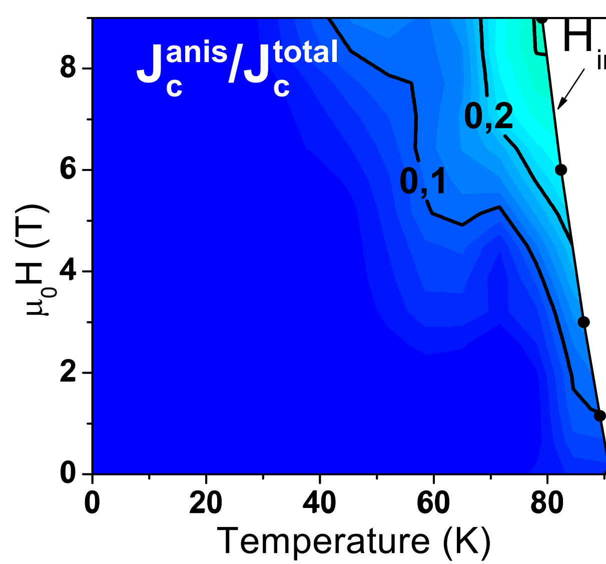

Conclusions and Outlook

- **Chemical solution deposition** is a versatile technique to generate artificial pinning structures. **Complementariry with PLD?**
- The methodology to analyze **vortex pinning contributions** can be **used for PLD nanocomposites.**
- **Interfacial nanostructures** are successfully grown by CSD and c-axis anisotropic defects are artificially introduced in YBCO films. **Can be combined with PLD?**
- CSD **nanocomposites** are very promissing, vortex pinning is controlled by strain generated by isotropic defects. **Strain in self-organized PLD nanorods?**
- **Magnetic nanostructures** have been introduced in YBCO films showing an enhancement of vortex pinning
- We need to use the **nanoscale imaging** methods to correlate vortex pinning with APC